
APPENDIX G**CONTAINMENT SYSTEM EVALUATION****TABLE OF CONTENTS**

	Page
G.1 CONTAINMENT SYSTEM DESCRIPTION.....	G.1-1
G.2 LEAK PATHS	G.2-1
G.3 SHIELD BUILDING VENTILATION SYSTEM ANALYSIS (SBVS-CODE).....	G.3-1
G.3.1 Reactor Containment Vessel Shell Temperature Evaluation....	G.3-1
G.3.2 Shield Building Ventilation System (SBVS) Analysis.....	G.3-2
G.3.3 Shield Building Ventilation System - Mathematical Model.....	G.3-2
G.3.4 Computational Details.....	G.3-3
G.3.5 Computational Procedure.....	G.3-11
G.3.6 Results and Discussion	G.3-12
G.3.7 Parameter Study	G.3-15
G.3.8 Conclusions.....	G.3-17
G.4 EVALUATION OF DOSES AND DOSE REDUCTION FACTORS	G.4-1
G.4.1 Comparison of Dose Calculations	G.4-1
G.4.2 Simplified Analysis of Dose Reduction Factors Associated with Dual Containment	G.4-2
G.4.3 Proposed Minimum Factors of Credit for Shield Building Effectiveness.....	G.4-7
G.5 MIXING ANALYSIS AND POSSIBLE MIXING TESTS	G.5-1
G.5.1 Significance of Mixing Assumptions in Dose Calculations	G.5-1
G.5.2 Mixing During Positive Pressure Period	G.5-2
G.5.3 Mixing During First Pass to Recirculation Inlet.....	G.5-4
G.5.4 Mixing of the Recirculated Component	G.5-5
G.6 SYSTEM TESTING.....	G.6-1

TABLE OF CONTENTS [Continued]**LIST OF TABLES**

TABLE G.2-1	LEAKAGE PATHS INTO SHIELD BLDG. FROM CONTAINMENT
TABLE G.2-2	THROUGH LINE LEAKAGE THAT BYPASS ANNULUS AND TERMINATES IN ABSVZ
TABLE G.2-3	THROUGH LINE LEAKAGE THAT BYPASSES BOTH ANNULUS AND ABSVZ
TABLE G.3-1	CALCULATIONAL BASES FOR SHIELD BUILDING MAXIMUM INTERNAL PRESSURE POST DBA
TABLE G.3-2	SUMMARY OF PARAMETER STUDY
TABLE G.3-3	TWO-HOUR DOSE AT SITE BOUNDARY
TABLE G.3-4	SHIELD BUILDING DISCHARGE AND RECIRCULATION FOLLOWING A LOSS-OF-COOLANT ACCIDENT
TABLE G.4-1	COMPARISON OF THYROID DOSE CALCULATIONS FOR NORMALIZED TOTAL CONTAINMENT LEAKAGE RATE OF .01/DAY, ALL DOSES IN REMS
TABLE G.4-2	COMPARISON OF WHOLE BODY DOSE CALCULATIONS FOR NORMALIZED TOTAL CONTAINMENT LEAKAGE RATE OF .01/DAY, ALL DOSES IN REMS
TABLE G.4-3	SIMPLIFIED REDUCTION FACTORS FOR 20 MINUTE TO 2 HOUR THYROID DOSE
TABLE G.4-4	SIMPLIFIED REDUCTION FACTORS FOR 20 MINUTE TO 2 HOUR WHOLE BODY DOSE
TABLE G.4-5	SHIELD BUILDING DISCHARGE AND RECIRCULATION FOLLOWING A LOSS-OF-COOLANT ACCIDENT

TABLE OF CONTENTS [Continued]**LIST OF FIGURES**

FIGURE G.3-1	CONTAINMENT DOME AND CYLINDRICAL WALL OUTSIDE SURFACE TEMPERATURE TRANSIENT
FIGURE G.3-2	CONFIGURATION WITHOUT RECIRCULATION
FIGURE G.3-3	CONFIGURATION WITH RECIRCULATION
FIGURE G.3-4	ANNULUS AIR TEMPERATURE
FIGURE G.3-5	ANNULUS PRESSURE (BOTH SBVS OPERATING)
FIGURE G.3-6	FLOW OUT OF SBVS (BOTH SBVS OPERATING)
FIGURE G.3-7	ANNULUS PRESSURE (33% LOWER H.T. COEFF.)
FIGURE G.3-8	FLOW OUT OF SBVS (33% LOWER H.T. COEFF.)
FIGURE G.3-9	ANNULUS PRESSURE (25% HIGHER H.T. COEFF.)
FIGURE G.3-10	FLOW OUT OF SBVS (25% HIGHER H.T. COEFF.)
FIGURE G.3-11	ANNULUS PRESSURE (SHIELD BUILDING LEAKAGE)
FIGURE G.3-12	FLOW OUT OF SBVS (SHIELD BUILDING LEAKAGE)
FIGURE G.3-13	ANNULUS PRESSURE - WITHOUT HEAT TRANSFER TO CONCRETE WALL
FIGURE G.3-14	FLOW OUT OF SBVS - WITHOUT HEAT TRANSFER TO CONCRETE WALL
FIGURE G.3-15	PRESSURE TRANSIENT IN THE ANNULUS - 2 SYSTEMS OPERATING
FIGURE G.3-16	FLOW OUT OF SYSTEM - 2 SYSTEM OPERATING
FIGURE G.3-17	WIND PRESSURE DISTRIBUTION

TABLE OF CONTENTS [Continued]

LIST OF FIGURES [Continued]

FIGURE G.3-18	PRESSURE TRANSIENT IN ANNULUS - 2 SYSTEMS OPERATING
FIGURE G.3-19	FLOW OUT OF SYSTEM - 2 SYSTEMS OPERATING
FIGURE G.3-20	CONTAINMENT PRESSURE TRANSIENT
FIGURE G.3-21	ANNULUS PRESSURE DESIGN BASIS TRANSIENT
FIGURE G.3-22	FLOW OUT OF SBVS DESIGN BASIS TRANSIENT
FIGURE G.5-1	AXISYMMETRIC FLOW DISTRIBUTION FROM A CIRCULAR JET
FIGURE G.5-2	AXISYMMETRIC FLOW DISTRIBUTION FROM A CIRCULAR JET

APPENDIX G – CONTAINMENT SYSTEM EVALUATION**G.1 CONTAINMENT SYSTEM DESCRIPTION**

The total containment consists of two systems:

- a. The Primary Containment System (see Sec. 5) consists of a steel structure and its associated Engineered Safety Features (ESF) systems. This system, also referred to as the Reactor Containment Vessel, is a low-leakage steel shell, including all its penetrations, designed to confine the radioactive materials that could be released by accidental loss of integrity of the Reactor Coolant System pressure boundary. ESF Systems directly associated with the Primary Containment System include the Containment Vessel Internal Spray, (Sec. 6.4) Containment Air Cooling, (Sec. 6.3) and Containment Isolation System (Sec. 5.2.2.1.1).
- b. The Secondary Containment System consists of the Shield Building, (Sec. 5.3) its associated ESF systems, and a Special Ventilation Zone, (Sec. 10.3.4) in the Auxiliary Building. The Shield Building is a medium-leakage concrete structure surrounding the Reactor Containment Vessel and designed to provide:
 1. Biological shielding for Design Basis Accident (DBA) conditions;
 2. Biological shielding for parts of the Reactor Coolant System (RCS) during operation;
 3. Protection of the Reactor Containment Vessel from low temperatures and other adverse atmospheric conditions, and external missiles;
 4. A means for collection and filtration of fission-product leakage from the Reactor Containment Vessel following the DBA. The Shield Building Ventilation System (SBVS) is the engineered safety feature utilized for this function.

The Special Ventilation Zone of the Auxiliary Building confines most leakage paths that could conceivably by-pass the Shield Building annulus. A small number of potential leakage paths could bypass the Shield Building Annulus and the Auxiliary Building Special Ventilation Zone. These leakage paths are accounted for in the dose analyses.

99064

99064

THIS PAGE IS LEFT INTENTIONALLY BLANK

G.2 LEAK PATHS

In this section the objective is to show that the probability for leakage from the primary containment to the Auxiliary Building is small compared with the probability for leakage to the Shield Building annulus.

This list of penetrations was arranged into eight groups to permit a detailed examination of the transport path of potential leakage from each group.

a. **GROUP I**

Leakage through valve seats associated with these penetrations is collected in the Waste Disposal System, which is a closed minimal leakage system normally maintained in good leak-tight condition since it is continuously handling radioactive effluents. Leakage from this group of penetrations does not get into the Auxiliary Building except by leakage through valve packing and any other mechanical joints. This will be minimal due to the type of valve used for this service, and the maintenance practices employed at the PINGP.

b. **GROUP II**

The leakage through seats from this group ultimately enters the volume control tank, which is designed to withstand 75 psig and operates normally as a gas-tight system. The volume control tank would normally remain in a pressurized condition following a loss-of-coolant accident, and could be vented to the Waste Gas System, if necessary. The check valves at the suction of the charging pumps provide the closed system boundary for the charging and seal injection penetrations. This closed system serves as a leakage collection boundary for the check valves inside of containment.

Although not vented to the volume control tank, Instrument lines are included in this group since they are self-closed lines.

c. **GROUP III**

Leakage through valves or seals associated with this group of penetrations is sealed by pressure which is normally higher than containment accident pressure.

d. GROUP IV

Leakage through valves or seals associated with this group of penetrations will enter the Shield Building annulus by special design of the isolation system.

With respect to the Hydrogen Control System air supply: During accident conditions and with the system not in use, the isolation valves inside and outside containment will be closed. Any potential leakage through valve seats will enter the Shield Building annulus through the opening that is provided in the line outside the isolation valves.

e. GROUP V

Leakage through valves or seals associated with this group of penetrations is stopped by a water seal:

1. With respect to the Fuel Transfer Tube: This tube is closed by a blind flange with double redundant gaskets located on the containment side of the tube and an isolation valve is normally under approximately 38 feet of water on the Auxiliary Building side. There will be no potential for leakage as soon as containment pressure is reduced to approximately 16 psig. This reduction in pressure will occur in the first few hours after the accident. Any small leakage during these first hours will pass through the water seal and the iodine will be scrubbed from the leakage. The flange (with double gaskets) is the credited isolation for this penetration.
2. With respect to Main Steam, Feedwater and Steam Generator Blowdown Systems: A pressurized water seal in the secondary side of the steam generators will be maintained by the Auxiliary Feedwater pumps so that these isolation systems will not leak containment atmosphere following the accident.
3. With respect to the Component Cooling System: These isolation valves are covered by a water seal established by the level of water in the Component Cooling System surge tank or by the discharge head of the component cooling pump.
4. With respect to the Cooling Water System: Isolation valves are provided for isolating a leaking fan coil unit. These valves are covered by water seal established by the discharge head of the Cooling Water pumps either directly or via a bypass line. Thus, to minimize containment leakage through these penetrations, the bypass valve is opened following the identification and isolation of the leaking unit.

f. GROUP VI

Leakage through valves and seals associated with this group of penetrations could bypass the Shield Building annulus and enter the Auxiliary Building.

Any leakage from this group is expected to be very small for the following reasons:

1. Most of the lines associated with these penetrations have small valves which are maintained in a leak tight condition.
2. Flanges associated with these penetrations are leak tested, following reassembly and are not normally disturbed during normal operation. It is reasonable to expect any leakage through these joints to be less than or, at worst, equal to measured test leakage.
3. Leakage from sample systems will be filtered through the sampling room filters.

g. GROUP VII

These systems are required to operate following a loss-of-coolant accident. The seals and packings of the equipment associated with those systems recirculating containment water will comply with the low-leakage requirements defined in Section 6.6. Leakage through the seals and packings will enter the Auxiliary Building Special Ventilation Zone. The activity from this leakage is discussed in Section 6.7.

Some of these systems are only operating for specific periods of time during post accident mitigation (e.g., Containment Spray). Valves in these systems are leak tested to ensure that, during non-operational periods, leakage to the Auxiliary Building through these penetrations will be minimal.

h. GROUP VIII

Leakage past the valve seat or seals is into the Shield Building.

Table 5.2-1 includes all penetrations. A further breakdown was made of the above information identifying the potential leak paths and where they terminate. Table G.2-1, lists the potential leakage paths to the Shield Building from Containment. Table G.2-2 lists the potential leakage paths to the Auxiliary Building Special Ventilation Zone. Table G.2-3 lists the through-line leakage that could bypass both the Shield Building and the ABSVZ. Penetration number in the Tables in this Appendix are applicable to Unit 1. Based on the above descriptions of the various groupings, penetrations in groups II, V, and VII, with the exception of the fuel transfer tube, are not included in these tables.

The potential leakage bypassing both the Annulus and the ABSVZ, based on a comparison of nominal seal or seat diameters, can be obtained from Table G.2-3. The total from this Table represents less than 5% of the total. Thus, the effect on dose will be minimal. The sensitivity of the bypass dose is shown in Section G-4 (historical information).

Leak Path Testing

Since the offsite dose consequence of where containment leakage is treated is of significance in this dual containment concept, provisions are made to determine, by test, how much containment leakage could bypass the annulus through various paths.

The Type B and C tests (Appendix J 10CFR50 terminology) identify leakage through individual leakage paths. Vents, drains and isolation valving are provided to allow testing of the potential leakage paths past valve seats, resilient seals and double wall expansion bellows. Valves will be tested by individually pressurizing or by pressurizing between valves and the leakage computed by pressure decay or metering. The volume between double seals or bellows will be pressurized, and the leakage rate will be metered, or the leakage rate computed by pressure decay.

G.3 SHIELD BUILDING VENTILATION SYSTEM ANALYSIS (SBVS-CODE)

The objective of this section is to show that the performance of Shield Building Ventilation System is not sensitive to reasonable variations in the analytical parameters and that all the parameters can be well defined from experimental data already published. This section provides the details of the SBVS model discussed in Section 5.3.2.

Section G.3 describes analyses (including tables and figures) performed for the Final Safety Analysis Report (FSAR). These analyses are strictly historical and have not been updated since the FSAR. No effort has been made to verify the information in this section. References to other sections of the safety analysis report within this section are applicable to the FSAR.

G.3.1 Reactor Containment Vessel Shell Temperature Evaluation

The free-standing Containment Vessel was designed to accommodate the maximum internal pressure that would result from the Design Basis Accident. For initial containment conditions typical of normal operation at 120°F and 14.7 psig, an instantaneous double-ended break with minimum safety features results in a peak pressure of 42.6 psi at 268°F. See Figure G.3-20.

Reference conditions for the Reactor Containment Vessel pressure transient are the operation of one spray pump and two fan coil units, with start-up at 60 seconds.

The margin in Containment Vessel design providing the capability for absorbing energy additions without exceeding the design pressure is discussed in detail in FSAR Section 14.3.4.

The heat transfer coefficient of the Reactor Containment Vessel internal surface was based on the work of Tagami.⁽¹⁾ From this work it was determined that the value of the heat transfer coefficient increases parabolically to a peak value at the end of blowdown and then decreases exponentially to a stagnant heat transfer coefficient which is a function of steam-to-air weight ratio. For details, refer to FSAR Section 14.3.4.

The CONTEMPT code has been used to determine the temperature transient of the Reactor Containment Vessel (CV) outer surface and the vessel peak pressure. Both temperature and pressure parameters are used as input for the SBVS analysis code. Each of these parameters was determined by using a separate set of conservative input data for the CONTEMPT code calculations. For determining the peak internal pressure of the CV a best estimate value of the inside surface heat transfer coefficient was used, and the calculated peak pressure was 42.6 psi. Additionally for SB annulus volume reduction calculations due to CV expansion a conservatively higher pressure of 46 psi was used. For determining the CV outer surface temperature transient an internal heat transfer coefficient 25% higher than the above best estimate value was used. This results in a conservatively higher shell temperature, as shown in Figure G.3-1. This temperature transient is then used for the SBVS analysis which incorporates additional conservatism.

G.3.2 Shield Building Ventilation System (SBVS) Analysis

The safety analysis is based on conservatively-chosen assumptions regarding the sequence of events relating to activity release, and attainment of vacuum in the Shield Building annulus, the effectiveness of filtering, the leak rate of the Containment Vessel as a function of time, and the mixing factor of fission products within the annulus volume.

The initial conditions and coefficients for the air in the Shield Building annulus are given in Table G.3-1.

G.3.3 Shield Building Ventilation System - Mathematical Model

The basic input or forcing function for this model is obtained from the Containment Vessel Pressure Temperature Transient. The mathematical model involves the following three transient phenomena, which interact with each other:

- a. Heat transfer from the steel shell to the air in the annulus; and that from the air to the concrete wall of the Shield Building, and that from the steel shell to concrete.
- b. Pressurization of the air in the annulus corresponding to the air temperature and air mass remaining in the annulus.
- c. The flow of air through the network of ducts, fans, valves and the charcoal filter system, along with the in- or out-leakage of air through the walls of the Shield Building. See Figures G.3-2 and G.3-3.

G.3.4 Calculational Details**a. Heat Transfer**

The simultaneous heat transfer from the surface of the steel wall to air and to concrete is given by the following differential equations:

$$W_a C_a \frac{dT_a}{dt} = h_L A_L (T_L - T_A) + h_U A_U (T_U - T_A) - h_c A_C (T_A - T_C) + H_f \quad (a)$$

$$W_c C_c \frac{dT_c}{dt} = h_c A_C (T_A - T_C) + H_c \quad (b)$$

Where:

- a. W_a : Instantaneous mass of air in the annulus.
- b. W_c : Mass of concrete involved in the heat up.
- c. T_A : Temperature of air.
- d. T_c : Temperature of concrete.
- e. T_L : Temperature of the lower (cylindrical) surface of the steel vessel.
- f. T_U : Temperature of the upper (dome) surface of the steel vessel.
- g. C_a : Specific heat at constant volume of air.
- h. C_c : Specific heat of concrete.
- i. A_L, A_U : The surface areas of the cylindrical part and the dome part of the steel vessel respectively.
- j. A_C : The surface area of concrete.
- k. H_f : Heat radiated from the steel surface to concrete directly. The usual Stefan-Boltzman law is applied to account for this term.
- l. H_f : Heat added to the air mass as a result of the additional heating (in the filter) of the recirculated air.

- m. h_U : Heat transfer coefficient for the dome surface to air transfer.
- n. h_L : Heat transfer coefficient for the cylindrical surface to air transfer.
- o. h_c : Heat transfer coefficient for the air to concrete transfer.

NOTE: h_U , h_L and h_c are all of the form

$$a(\Delta T)^b$$

where a and b are constants, and ΔT is the temperature difference between the media.

Solution of the heat transfer equations

The procedure used to solve equations (a) and (b) of the mathematical model is given below. The equations are solved simultaneously for any time increment. Since the time increment, Δt , considered are very small (typically, .05 sec.) the coefficients in the equations are essentially constants during each increment. They are updated after each increment of time. The effects of the terms H_f and H_r are small and hence, they can be introduced as a correction to T_A and T_c after they have been computed assuming H_f and H_r to be absent in the equations.

Under these assumptions, equations (a) and (b) are incrementally linear, and hence, the values of T_A and T_c at the end of any time interval can be obtained if their values at the beginning of the time increment are given, along with the variation of T_L and T_U with respect to time.

The solution is obtained by using the well known technique involving Laplace transformation.

The solution to the values of T_A and T_c at the end of any Dt , denoted by T_{A2} and T_{c2} can be written as follows:

$$T_{A_2} = A_0 + A_1 e^{s_1 \Delta t} + A_2 e^{s_2 \Delta t} \quad (c)$$

and

$$T_{c_2} = B_0 + B_1 e^{s_1 \Delta t} + B_2 e^{s_2 \Delta t} \quad (d)$$

where $A_0, A_1, A_2, S_1, S_2, B_0, B_1, B_2$ are functions of the independent variables or coefficients in the list following Equations a and b.

b. Heat Transfer Coefficients

The heat transfer rate from the shell to the air was evaluated with consideration for both natural convection heat transfer and heat transfer by radiation. The convective heat transfer was evaluated using the equation for natural convective heat transfer recommended by many investigators. ⁽²⁾

$$N_{Nu} = c [N_{Gr} N_{Pr}]^n$$

where, in the turbulent region,

$$c = 0.14$$

$$n = 1/3$$

N_{Gr} – Grashof Number

N_{Nu} – Nusselt Number

N_{Pr} – Prandtl Number

Appropriate substitution of the physical parameters produced the following heat transfer equations:

For vertical walls (external surface)

$$h_c = 0.196 (\Delta t)^{1/3} \quad (G.3-2)$$

For the Shield Building dome (internal surface)

$$h_c = 0.224 (\Delta t)^{1/3} \quad (G.3-3)$$

For the Containment Vessel hemispherical head (external surface)

$$h_c = 0.205 (\Delta t)^{1/3} \quad (G.3-4)$$

The above natural convection heat transfer coefficients are temperature (therefore time) dependent variables in the computer model. In addition, these are the coefficients that were varied in the parameter study as explained later in Section G.3.7.

The radiative heat transfer was evaluated using the classical equation:

$$h_r = \frac{0.1384 \left[\left(\frac{T_w}{100} \right)^4 - \left(\frac{T_c}{100} \right)^4 \right]}{(T_w - T_c)} \quad (G.3-5)$$

Where:	T_w	=	Reactor Containment Vessel outside surface (the surface facing the annulus air) temperature (°R)
	T_c	=	Shield Building Concrete inside surface temperature (°R)
	0.1384	=	A factor which includes an emissivity factor of 0.8 and the Stefan-Boltzman Constant.

Due to the low temperatures involved in the analysis the radiation contribution is very small in the total heat transfer interactions. Nevertheless, its effect is included in all of the transient analyses.

c. Pressurization of the Air in the Annulus

The change in the annulus air pressure due to thermal effects is obtained by assuming that the air is an ideal gas and applying the ideal gas equations in differential form:

$$\frac{dP_a}{dt} = \frac{R}{V} \left[T_a \left(\frac{dW_a}{dt} \right) + W_a \left(\frac{dT_a}{dt} \right) \right] \quad (G.3-6)$$

Where:

P_a	=	the pressure of the annulus
V	=	volume of the annulus
R	=	gas constant for air
W_a	=	weight of air in the annulus
t	=	time
T_a	=	absolute temperature of the annulus air (°R)

d. Flow of Air Through the Shield Building Ventilation System

The assumption made was that the fans run at a constant speed, so that the inertial effects of the fans can be neglected. Also, the transport lag effects are assumed negligible. As a consequence, the air flow through the ducts can be calculated using the instantaneous values of the annulus pressure and the steady state characteristics (pressure drop versus flow rate) of the fans. The flow through the ducts can be obtained by solving a set of simultaneous, nonlinear, algebraic equations describing the conservation of momentum in the vent system. The solution of these algebraic equations has the constraint that the presence of the check valves does not allow flow in the negative direction (no flow of atmospheric air into the system).

The pressure drop ΔP_d , through any duct has the following general form:

$$\Delta P_d = c_1 \times L \times Q^{c_2} \quad (G.3-7)$$

Where:

L	=	the equivalent length of duct (in 100's of feet)
Q	=	the flow rate
And c_1, c_2	=	constants.

The fan characteristics, namely, the pressure head, ΔP_f , versus flow rate, Q , are given as polynomial relationships as follows:

$$\Delta P_f = a_0 + a_1 Q + a_2 Q^2 + a_4 Q^4 \dots \quad (G.3-8)$$

where the coefficients a_0, a_1, \dots are obtained by a curve fitting procedure involving the minimum mean square error criterion.

The pressure drop through the charcoal filter, ΔP_{cf} , is expressed as

$$\Delta P_{cf} = c_3 Q^{c_4} \quad (G.3-9)$$

where c_3 and c_4 are constants, and Q is the flow rate through the filter.

The pressure drop through the control valves, ΔP_v , is obtained as:

$$\Delta P_v = \left(P_1 \pm \sqrt{P_1^2 - 4cQ_v^2 T} \right) \div 2 \quad (G.3-10)$$

where P_1 is the air pressure at the entrance to the valve, (psia)

Q_v	=	the flow rate of air
T	=	temperature of the air (absolute)
c	=	a constant.

The flow path in the ventilation system has two configurations, namely, with and without recirculation. Figures G.3-2 and G.3-3 represent these configurations.

In these figures, B fan and S fan represent a large and a small fan respectively. These fans operate in parallel. After the transient heating subsequent to the LOCA has subsided (after several minutes), a smaller fan is capable of maintaining a small negative pressure in the annulus.

The numbers 1, 2, 3, 4, 5, and 6 are used to identify the corresponding sections of the vent system; XT (1), . . . XT (6) represent the flow rates in these sections. Let $\Delta P_1, \Delta P_2 \dots \Delta P_6$ represent the pressure drops in the sections as a result of friction, the presence of the filter (only for section 1), and the pressure drops across the valves. ΔP_B and ΔP_S represent the respective pressure heads generated by the large and small fans. All of the above pressure increments are nonlinear functions of the corresponding flow rates.

The following are the nonlinear equations used to solve for the flow rates:

Equations for flow rates without recirculation (assuming the outdoor gauge pressure to be zero)

$$P_A - \Delta P_1 - \Delta P_2 + \Delta P_B - \Delta P_6 = 0 \quad (G.3-11)$$

$$\Delta P_B - \Delta P_2 = \Delta P_S - \Delta P_3 \quad (G.3-12)$$

$$XT(1) = XT(2) + XT(3) \quad (G.3-13)$$

$$XT(4) = XT(2) \quad (G.3-14)$$

$$XT(6) = XT(3) + XT(4) \quad (G.3-15)$$

Equations for the flow rates with recirculation

$$P_A - \Delta P_1 - \Delta P_2 + \Delta P_B - \Delta P_6 = 0 \quad (G.3-11)$$

$$\Delta P_B - \Delta P_2 = \Delta P_S - \Delta P_3 \quad (G.3-12)$$

$$XT(1) = XT(2) + XT(3) \quad (G.3-13)$$

$$XT(6) = XT(3) + XT(4) \quad (G.3-15)$$

$$P_A + \Delta P_5 - \Delta P_6 = 0 \quad (G.3-16)$$

$$XT(5) = XT(2) - XT(4) \quad (G.3-17)$$

01436316

Where:

P_A	=	Pressure in the annulus.
ΔP_1	=	Pressure drop from the annulus to the suction of the two fans (includes duct and filter).
ΔP_2	=	Pressure drop from the discharge of the recirculating fan (Big Fan) to the discharge vent (includes all ducting and valves in the line).
ΔP_3	=	Pressure drop from the discharge of the exhaust fan (Small Fan) to the discharge vent (includes all ducting and valves in the line).
ΔP_5	=	Pressure drop from the discharge of the recirculating fan to the annulus, including all recirculating ducting and valves.
ΔP_6	=	Pressure drop, discharge vent to the atmosphere.
ΔP_B	=	Pressure head generated by the recirculating fan.
ΔP_S	=	Pressure head generated by the exhaust fan.
XT(1)	=	Flow through the filter assembly.
XT(2)	=	Flow through the recirculating fan.
XT(3)	=	Flow through the exhaust fan.
XT(4)	=	Exhaust flow from the recirculating fan.
XT(5)	=	Recirculation flow to the annulus.
XT(6)	=	Total exhaust flow to the atmosphere from the discharge vent.

The systems are actuated by the Safety Injection Signal, with both of the fans initially at rest and all valves closed. After 36 seconds (this time is governed by the loading sequence on the diesel generator plus conservative evaluation) the fans are turned on, and the discharge valves opened. The annulus pressure then decreases and goes to a set-point negative value (-2.0" of water), which provides a signal for opening of the recirculation valve.

G.3.5 Computational Procedure

The equations of the mathematical model are solved by discretizing the independent time variable. It is clear that the equations are coupled, and therefore care must be taken while decoupling them for the digital solution. The equations for the flow through the system are algebraic; hence, the dependent variables in these equations are taken as the mean value for the corresponding time increment. Since the time increments chosen are small, an average of these values between the beginning and the end of the time increment is considered to be adequate to represent the mean value.

The following are the basic steps in the computation for any time increment.

1. Starting from the temperatures of the air and concrete at the beginning of a time step, the conservation of energy equations (two differential equations) are used to solve simultaneously these temperatures at the end of the time step, corresponding to a given rise of surface temperature of the Reactor Containment Vessel. The air pressure corresponding to the temperature is calculated using the perfect gas law.
2. The following logic dictates whether the recirculation path is open or closed. The path is closed during the initial portions of the transient when the annulus pressure is above the set point of -2" of water. The recirculation path is opened (at the end of the time step) when the average annulus pressure drops below the set point. The average annulus pressure is defined as the average of the initial and final pressure for any time step.
3. Using the air flow paths in action, a consistent set of flow continuity and pressure drop equations involving fan characteristics and duct losses are used to evaluate the flow rate through each of the paths corresponding to the average annulus pressure.
4. The annulus air mass is adjusted, using the net amount of air removed from the annulus during the time increment. The amount of air removed is computed from the above flow rates, the leakage rate from the vessel into the annulus, and the leakage rate from or to the atmosphere.
5. The annulus air temperature is adjusted to account for the higher temperature of the recirculated air, and the concrete temperature is adjusted to account for the direct radiative transfer of heat from the Reactor Containment Vessel.
6. A correction for the annulus air pressure, corresponding to the correction for the annulus air mass and correction for the air temperature, as mentioned in Steps 4 and 5 above is now applied, and this corrected pressure is taken as the annulus pressure at the end of the time increment

The above calculational steps are repeated for each time increment, printing out the needed results. The corrections in Steps 4, 5, and 6 are extremely small compared to the changes involved during the corresponding time steps. The correction has never been more than 1%. But for this fact, the above equations would have to be solved by iteration.

G.3.6 Results and Discussion

Analyses were made considering the instantaneous expansion of Reactor Containment Vessel due to the blowdown pressure transient. This causes the annulus volume to decrease by 2450 ft³, thereby causing a concurrent rise in annulus air pressure of 2.7" of water column (W.C.).

The reference or design basis analysis is shown on Figures G.3-21, G.3-22 and G.3-4. From Figure G.3-21, it can be seen that the annulus pressure rises to 2.7" W.C. instantaneously due to the shell expansion and then rises slowly to 3.0" W.C. due to the thermal transient (for 36 seconds). At this time the SBVS is in operation and, for the analysis, it is assumed one of the two systems fails to operate. The annulus pressure reaches zero at about 2.6 minutes, and continues to decrease further. At about 4.0 minutes, the annulus reaches a pressure of -2.0" W.C. and the recirculation starts. During this time interval (36 seconds to about 4.0 minutes) both of the fans are in full exhaust mode.

After the opening of the recirculation valve, the annulus pressure rises again (the thermal transient is still in progress). A little after 5 minutes the fan capacity overtakes the thermal expansion effects and the annulus pressure once again decreases.

A pressure of -2.0" W.C. was chosen to start recirculation so that for any significant variations in system parameters, the pressure in the annulus (after initiation of recirculation) remains negative for remainder of the DBA. During this period, the recirculating fan is in a dual mode. Initially, a large portion of the fan discharge flow is exhausted to the discharge vent and a small portion is circulated back into the annulus. This ratio of exhaust to recirculation flow from the recirculation fan decreases continually for about 20 minutes, at which time it reaches zero. The fan characteristics and duct losses are such that at this time, the small fan is in full exhaust mode. The total flow out of the system follows the same pattern and is shown on Figure G.3-21. The system reaches a pressure of -3.25" W.C. in 20 minutes. The steady state exhaust flow is 180 cfm.

The annulus air temperature transient is shown in Figure G.3-4.

Both transient and steady state results calculated by the computer codes have been verified by hand calculations.

The parameters used in the SBVS analysis are derived from well known literature sources and appropriate safety analyses which employ conservative assumptions - not "best estimate" values. This is followed by investigation of the conservatism involved in varying each parameter in either direction. The advantage of such an approach is limited by the difficulty in relating such effects to dose consequences, because the dose calculation in itself is a complicated and necessarily separate aspect of the overall calculation.

The course followed has been to determine a conservative input to the dose calculation on the basis of an envelope of results from the Shield Building calculation, with the intent of embracing the worst consequences resulting from reasonable variation of the Shield Building parameters in either direction.

1. Shell Temperature:

The outer surface temperature of the containment vessel is predicted from the CONTEMPT Code, which assumes the outer surface is insulated. Analysis has shown that the outer surface temperature is rather insensitive to the value selected for the condensation heat transfer coefficient of the inside surface. For example, with an inside heat transfer coefficient 25% higher than the Tagami value the outside surface peak temperature and convective heat transfer coefficient are only higher by 7.4% and 6.1% respectively. A 100% higher value of the inside heat transfer coefficient (peak value of 650 Btu/hr-ft²-°F) only increases the outside surface temperature and convective heat transfer coefficient by 12.2% and 10.1% respectively. Since Tagami's⁽¹⁾ value of the inside heat transfer coefficient has been given support experimentally as reported by Slaughterbeck⁽³⁾ it is not believed reasonable to use Kolflat's⁽⁴⁾ arbitrarily selected values starting at a peak of 620 Btu/hr-ft²-°F and decreasing linearly to 40 Btu/hr-ft²-°F in 25 seconds. The 25% higher heat transfer coefficient value has been used in all the calculations.

The LOCA temperature transient inside the Containment Vessel is that associated with a double ended break (DBA). This provides input to compute the outer surface temperature. Calculations of the temperature of the outer surface of the containment vessel following smaller breaks indicates that the double ended break provides the most severe temperature transient.

2. Heat Transfer to Annulus Air

The effect of larger outer surface heat transfer coefficients has been explored far beyond reasonable upper limits and for somewhat less than nominal conditions. A 25% larger coefficient appears to be a reasonable upper limit.

3. Shield Building Leakage

The amount of Shield Building leakage is inversely proportional to the time required to achieve negative pressure. From the standpoint of dose, the faster that negative pressure is obtained, the lower the released dose. However, the larger the in-leakage rate, the more the recirculation mode is delayed and this also reduces the recirculation ratio, which consequently gives less dose attenuation during the recirculation phase. The dose calculation is based on an outflow corresponding to a high out-leakage during the positive pressure period ignoring the actual time the system requires. The calculations also apply a conservatively high in-leakage rate during the rest of the time period.

4. Wind Velocity

One of the functions of the SBV system is to achieve and maintain sufficient negative pressure at all points within the annulus to preclude exfiltration as a consequence of external wind conditions.

The effect of as much as 1/4 inch displacement of the pressure curves (a 40 mph wind equivalent) shows essentially no effect on the time at positive pressure.

A wind effect applied at the stack, but not at the in-leakage sources, could result in some increase in discharge flow, but this would be compensated by increased atmospheric dispersion.

5. Outside and Annulus Air Temperature

The initial ΔT between the Containment Vessel atmosphere and the annulus will influence the annulus pressure transient.

For example, under some operating conditions the Containment Vessel atmosphere is 80°F. For, outside temperatures less than 80°F, the annulus air temperature will be some place between the two values. These conditions could lead to a slightly longer positive pressure period.

The dose calculations assume a 4.5 minute positive pressure period to accommodate the effect of different initial conditions even though the design basis period is only 2.6 minutes.

An analysis was previously made to demonstrate that the structural integrity of the Shield Building could not be endangered by pressurization resulting from any malfunction of the SBVS.

However, in the context of a safety analysis it is appropriate to assume in the unlikely event of a LOCA, that one of the two redundant trains of the SBVS is operable, and that finite leakage from the annulus occurs. Therefore, a 2 psig internal pressure in the Shield Building, resulting from failure of both trains of the SBVS, combined with no out-leakage or heat loss is not assumed to be a credible situation.

A conservative calculation of the maximum positive pressure in the Shield Building is 0.108 psi (3.0 in. W.C.). This pressure is 3.6% of the 3 psi pressure. The initial conditions, assumptions, and other parameters are identical to those used in the DBA analysis, FSAR Section 14.3.

G.3.7 Parameter Study

Further analysis beyond the design basis was directed to the investigation of the sensitivity of the performance of the system to changes in the reference parameters.

a. Operation of Both Shield Building Ventilation Systems

The transient for both Shield Building Ventilation Systems in operation are shown in Figure G.3-5 and G.3-6. The transient is very similar to the design basis analysis; however, the steady state pressure is lower (about - 3.25" W.C.), with a flow of 280 cfm. This is as expected because of increased in-leakage, due to the lower value of the annulus pressure.

b. Heat Transfer Coefficient Variation Study

The heat transfer coefficients from the external surface of the Reactor Containment Vessel to the air in the annulus are derived from well-established experimental data as detailed in reference 2, equations G.3-1 to G.3-4. The linear velocity of air flow in the annulus is of the order of less than 0.5 ft/min and therefore justifies the use of natural convection coefficients. The scatter of the experimental data as presented by several investigators in McAdams is less than $\pm 10\%$. However, recognizing the fact that the reactor environment is not identical to those under which the experiments were conducted, the heat transfer coefficient was varied from a realistic upper limit of 125% of the normal value to a lower limit of 67%.

The system performance for the various values of the heat transfer coefficients are shown in Figures G.3-7 through G.3-10. The lower heat transfer coefficient results in a lower positive pressure peak of 2.85" W.C. (Figure G.3-7) and reaches zero earlier than the design basis analysis, at about 1.5 minutes. The higher heat transfer coefficient results in a higher positive pressure peak of 3.2" W.C. (Fig. G.3-9) and a longer time to reach zero pressure (3.8 minutes).

The flow out of the systems follow a similar pattern. In all cases, however, steady state pressure and the total integrated flow out of the system are approximately the same as for the design basis transient.

c. Variation of Leak Characteristic of the Shield Building

In all of the above transient studies an assumed leak characteristic of the Shield Building as shown in Figure 5.2-8 and Table 5.2-5 of the FSAR were used. This value was 10% per day of the annulus volume at 1/4" W.C. differential pressure. (See Figure 5.2-8 of the FSAR, curve labeled "used for off-site dose calculation").

Analyses were made with arbitrary increases in the leak rate up to 100% day and are shown on Figures G.3-11 and G.3-12.

d. Additional Analysis

The design basis analysis was re-evaluated assuming the concrete as an adiabatic surface. In other words, no heat transfer was allowed into the concrete. The results are shown in Figure G.3-13 and G.3-14. The effect on the system performance is small, and as seen from Figure G.3-13 results in a longer positive pressure duration (4.7 minutes).

Four additional analyses were made using the following assumptions, both for one system and two systems based on a Shield Building leak rate of 1.0%/day and a Shield Building leak rate of 10.0%/day:

- a. 25% higher heat transfer from steel shell to annulus air
- b. 25% lower heat transfer to concrete
- c. Initial temperature of air in the annulus of 50°F and ambient of -20°F
- d. Initial temperature of air in the containment 80°F
- e. A wind of 40 mph at the outside of the Shield Building.

The results of these analyses are shown on Figures G.3-15 and G.3-16, G.3-18 and G.3-19.

The wind effect was assumed as a constant initial rise in annulus pressure of 0.735" W.C. Together with the instantaneous expansion of the vessel results in a positive pressure of 3.435" W.C.

The wind distribution is shown on Figure G.3-17.

The two-hour dose at site boundary is shown in Table G.3-3 which is based on shield building discharge shown in Table G.3-4.

G.3.8 Conclusions

It is concluded from these analyses that the SBVS, as designed, is capable of performing its intended function over a wide range of system parameters. The resulting two-hour dose at the nearest site boundary, as is shown in Section G.4, is significantly lower than the 10CFR100 guidelines.

A complete list of parameters and the resultant transients are given in Table G.3-2.

REFERENCES - Appendix G

Section G.3

1. Tagami, Tasaki, "Interim Report on Safety Assessments and Facilities Establishment Project in Japan for period ending June 1965 (No. 1)."
2. McAdams, W. H. Heat Transmission, 3rd Ed. 1954
3. Slaughterbeck, D. C., "Review of Heat Transfer Coefficients for Condensing Steam in a Containment Building Following a Loss of Coolant Accident", IN-1388, Sept. 1970. Idaho Nuclear Corporation, Idaho Falls, Idaho.
4. Kolflat, A., and Chittenden, W. A., "A New Approach to the Design of Containment Shells for Atomic Power Plants", Proc. of Am. Power Conf., Vol. 19 (1957).

THIS PAGE IS LEFT INTENTIONALLY BLANK

G.4 EVALUATION OF DOSES AND DOSE REDUCTION FACTORS

Section G.4 describes analyses (including tables and figures) performed for the Final Safety Analysis Report. These analyses are strictly historical and have not been updated since the FSAR. No effort has been made to verify the information in this section. References to other sections of the safety analysis report within this section are applicable to the FSAR.

99066

The objectives of this section are:

1. to compare in detail the results of dose calculations for the reference basis and for specific bases of evaluation suggested by the Commission.
2. to demonstrate the factors of dose reduction implicit in the dose calculations for the dual containment and the effects of mixing assumptions on these factors.
3. to propose certain minimum factors of dose reduction for purposes of evaluation.

G.4.1 Comparison of Dose Calculations

Tables G.4-1 and G.4-2 present the detailed dose comparison requested by the Commission with total containment leakage rate normalized to an initial one percent per day, followed by one-half percent per day beyond 24 hours.

The first column in each table corresponds to the reference case described in Section 14, except that 11 percent of the containment leakage is now assumed to bypass the Shield Building - 10 percent through the filters of the special ventilation zone of the Auxiliary Building plus one percent unfiltered bypass directly to the atmosphere. These bypass leakage values are regarded as conservative upper limits, and no credit is taken for mixing in the auxiliary building volume, although substantial reduction in this document of the two-hour dose would be expected as a result of the mixing holdup and deferred release of activity.

Column 2 in both tables is the same reference case adjusted for 90 percent filter efficiency rather than 95 percent.

Column 3 is the AEC suggested basis of evaluation wherein 70 percent of the containment leakage is arbitrarily assumed to be transported directly through the filters of either the Shield Building or the special ventilation zone. In this case, it is again assumed that 10 percent filtered release and one percent unfiltered release bypass the Shield Building, and that 59 percent, the remainder of the suggested 70 percent, is transported directly to the filters of the Shield Building. The remaining 30 percent is treated on the adjusted reference basis described by the second column.

The 59 percent component is assumed to experience only direct filter reduction for the first 20 minutes but the effects of recirculation are included beyond this time, still with no mixing or dilution on the first pass to the filter. As will be shown subsequently, the large advantage factors associated with recirculation are, at least for thyroid doses, largely independent of mixing in the first or subsequent passes, so there is no reason to neglect this advantage under the suggested basis of evaluation.

The last column in each table corresponds to an equivalent single containment with all but 1 percent of the Halogens released through a 90 percent filter, except during the first 4.5 minutes associated with positive annulus pressure, during which time it is assumed that all leakage to the Shield Building bypasses the filter. This column represents the theoretical dose potential which, as the other columns in the Tables demonstrate, can be greatly reduced by the effectiveness of the dual containment.

G.4.2 Simplified Analysis of Dose Reduction Factors Associated with Dual Containment

For purposes of recognizing and evaluating specific reduction factors that are implicit in the calculation of the dual containment performance, it is useful to consider simplified analyses that neglect decay and containment depletion, and thereby more clearly demonstrate the significance of the assumptions applied with regard to mixing.

The relevant factors are conveniently considered in terms of the dose intervals identified in Tables G.4-1 and G.4-2 for thyroid and whole body doses. The factors considered are the reductions applicable to the potential doses for each interval as listed in the last column of each table.

a. Initial Unfiltered Dose from Shield Building Outleakers

The reference calculation for the assumed initial 4.5 minute period of positive pressure assumes that mixing occurs in half the annulus volume. The equations for the annulus activity, A_2 , and the activity released to the environment during this period, A_3 , can be simplified by neglecting decay and leakage depletion in both the containment and the annulus.

$$A_2 = L_1 A_{10} t$$

$$A_3 = L_{D_0} \int_0^t A_2 dt' = L_D L_1 A_{10} \frac{t^2}{2} = L_1 A_{10} t \times \frac{L_D t}{2}$$

The first term in A_3 is the leakage into the annulus during the assumed 4.5 minutes which, for $L_1 = .0089/\text{day}$ (.01/day total leakage), represents a potential thyroid dose of 185 rem. This dose potential varies with time at positive pressure, while the calculated attenuated dose varies as time squared as a result of the increasing outleakage concentration.

The Shield Building attenuation is given by the second term, where a reduction in volumetric capacitance can be applied to L_D , the fractional leakage rate of the Shield Building, in the form of a participation factor, F . the reciprocal of the reduction is then:

$$\frac{2f}{L_D t} = \frac{2 \times f}{1.20 / \text{day} \times (4.5 / 1440 \text{ days})} = 532 f$$

For $f = 0.5$, the reduction would be 266, resulting in an unfiltered dose of $185/266 = 0.69$ rem.

Determination of the effect of very low participation factors requires that the effect of annulus depletion be included. The depletion can be considered as being only by outleakage or by outleakage plus filtered stack discharge, as in the reference calculation from 36 seconds to 4.5 minutes.

The 4.5 minute dose reduction factors in each case would vary as follows with participation factor, where L_2 , is taken as 23.1/day (6000 cfm) and $L_D = 1.2/\text{day}$.

f	Reduction in Unfiltered Dose	
	without competing stack release	with 6000 cfm stack release
1	534	545
.5	267	278
.1	54	64
.05	27	30
.01	6	22
0	1	19

Past evaluation of a similar Shield Building for the Sequoyah plant* has resulted in recognition of a reduction factor of 10 applied to thyroid dose during the period of positive pressure, with indication that further credit might result if appropriate tests were performed.

According to the above table, a factor of ten reduction in thyroid dose would correspond to a participation factor of only .018, or would be less than the minimum reduction where competitive removal by filtered stack release is considered. Conversely, it may be concluded that full mixture in only one fiftieth of the annulus volume (for example, in a vertical pie-shaped slice that is one-fiftieth of the circumference) should accomplish at least a tenfold reduction in thyroid dose.

* Docket 50-327: PSAR, Section 14.3.5; and AEC Safety Evaluation, Item 11.2, March 24, 1970.

The unfiltered outleakage component is unimportant with regard to whole body dose during this interval because the whole body dose is then essentially all due to the greater volume of stack release. The reduction factors applicable to the total whole body dose would be those in the first column above, but it is more convenient to consider a factor applicable over the larger interval of zero to 20 minutes, as in the next section.

b. Filtered Release from 0 to 20 Minutes

The reference calculation of filtered Shield Building release from time zero to twenty minutes is based on a stepwise reduction of exhaust flow from the annulus, as described in Table G.4-5. All flow is assumed to be directly out the filter, with no recirculation. Mixing during the single-pass transport to the vent system inlet duct is again assumed to occur in half the annulus volume ($f = 0.5$).

A reduction factor directly applicable to the 0 to 20 minute containment leakage properly includes that portion of the 20 minute annulus inventory released between 20 minutes and two hours, and the dose from this deferred component depends on the assumptions applied during the recirculation process beyond 20 minutes. The variation in reduction factor with participation factor is indicated in the following table where the same participation factor is assumed to apply during the later recirculation period, with 90% filtering of iodine.

f	Dose Reduction Factor		
	Neglecting later release of 20 minute inventory	Thyroid, including deferred release	Whole Body, including deferred release
1	26	15	11
.5	13	9	6
.1	3.5	3.1	1.7

The effect of noble gas decay significantly increases the whole body dose reduction factor associated with the larger participation factors; a reduction of 60 obtains at $f = 0.5$, with deferred release neglected, as may be noted from comparison of Columns 2 and 4 in Table G.4-2.

c. Filtered Release During Recirculation Phase

The most significant reduction factor is that associated with the 20 minute to 2 hour interval when recirculation is assumed to be established and when the effectiveness of mixing is least questionable.

Thyroid Dose

Direct release of .0089/day leakage (.01/day total) during this period would result in 391 rem thyroid dose with a 90 percent filter. The reference calculation assumes mixing with effectively half the annulus capacitance available, which reduces the dose by a factor of about 32 and results in a thyroid dose of 12.3 rem for the 90 percent filter.*

The source of this thyroid dose reduction factor can be understood more readily by neglecting decay, source depletion and initial inventory, and by solving directly for a reduction factor under various assumptions. Table G.4-3 compares the effects of different assumptions using these simplifications and somewhat simpler terminology than is used in Section 14. The last column on this chart presents the expression for the reduction factor relative to the case of direct filtered release, and gives numerical values for the case of 0.5 participation factor.

The case for the "actual flow pattern" in Table G.4-3 corresponds to the reference calculation. The thyroid dose reduction factor is the recirculation ratio, R , or its reciprocal, 20, times a capacitance factor associated with 100 minutes of recirculation flow, for a total reduction of 32. Reduced mixing, or lower participation factor, affects only the capacitance term in this case, so a reduction factor of at least $20 \times .915 = 18.3$ is applicable.

This same result permits direct calculation of a reduction factor applicable to the suggested composite halogen source (90 percent particulates and inorganics removable with 90 percent efficiency plus 10 percent organics removable with only 70 percent efficiency). The resulting reduction factor varies from 30 at a participation factor of 0.5 to 17 at low participation factors.

* The reference calculation for this time interval includes also the effects of partial release of the initial 20 minute inventory in the annulus, which causes typically 20 to 30 percent of the dose from the fresh component. This deferred component should be charged to the previous period and must be neglected in defining a reduction factor applicable to the containment leakage that occurs during the recirculation period.

A second way in which adverse mixing effects can be allowed for in the calculation is to neglect mixing of containment leakage until it has once passed the filter and begun to recirculated, as represented by the next case in Table G.4-3. This effect is shown to still result in a reduction factor of about 20. Neglect of the capacitance term in this case (or the assumption of very low participation factor) is equivalent to cascading the recirculated component through the filter such that a fraction $(1-n)$ escapes on first pass, a fraction $(1-n)(1-R)$ times as much escapes on second pass, $(1-n)^2(1-R)^2$ as much on third pass, etc., for a total release rate of $(1-n)[1-(1-n)(1-R)]$. The resulting Shield Building attenuation factor would then be 18 for a 90 percent filter and 19 for a 95 percent filter.

The significant conclusion that can be drawn from comparison of these two cases is that a minimum reduction factor that is approximately equal to the recirculation ration applies to the thyroid dose independent of the degree of mixing in either the first or subsequent passes. Over longer periods, as for the 30 day thyroid dose, the same factor also applies.

Based on these considerations, it is believed that a reduction factor of at least twenty is applicable to the thyroid dose during the recirculation period - in addition to the effect of direct discharge through a filter. Such a factor, equal to the ration of recirculation flow to discharge flow, is equivalent to the recirculation credit that has been recognized for the standby gas treatment system of a boiling water reactor plant (e.g., see Safety Analysis for Shoreham, Docket 50-322, Feb. 20, 1970).

Whole Body Dose

Table G.4-4 describes similar simplified reduction factors for the dose from noble gases during the 20 minute to two hour recirculation period with the effects of decay again neglected.

The effective capacitance of the annulus in these cases is seen to be based on discharge flow rather than recirculation flow, and the 100 minute dose reduction factor is 10 to 19 for a participation factor of 0.5, depending on whether or not first pass mixing is credited. The effect of reduced participation factor can be directly calculated. For example, with a participation factor of only 0.2, the dose reduction is 9.2 with credit for first pass mixing and 6.0 without such credit.

Larger reduction factors result when decay is considered. A factor of 26 may be inferred from comparisons of Columns 2 and 4 of Table G.4-2, where Column 2 includes also partial release of the 20 minute inventory and therefore leads to an underestimate of the reduction factor applicable to this time interval.

G.4.3 Proposed Minimum Factors of Credit for Shield Building Effectiveness

On the basis of the previous discussion, certain minimum factors of dose reduction might be associated with the effectiveness of the Shield Building, the application of which seems warranted even in the absence of mixing tests. Suggested values for these factors and their application to the potential doses described in Column 4 of Tables G.4-1 and G.4-2 result in the following adjusted doses for a nominal initial leak rate of .01/day.

Dose Component	Minimum Credit	Adjusted Thyroid Dose, rem	Adjusted Whole Body Dose, rem	
<u>Shield Building</u>	10	18.4	----	99064
0-4.5 min. unfiltered leakage	3.1 - thyroid 1.7 - whole body	20.3	6.1	
0-20 min. filtered release	20 - thyroid 6 - whole body	19.6	6.4	99064
20 min-2 hr. recirc. release				
Total Shield Building		58.3	12.5	
<u>Auxiliary Building</u>		53.0	5.6	
<u>Direct Leakage</u>		53.0	.5	
Total 2 hour dose		164.3	18.6	
<u>Total 2 hour dose using safety guide 4 Meteorology Values</u>		174	19.7	

At least two of the proposed credits have precedent, and all appear more than justified on a technical basis, as summarized in the following brief discussion of each item.

a. Positive Pressure Period

Full mixing in only one-fiftieth of the annulus results in at least a ten-fold reduction in direct thyroid dose during this period, which factor has previously been recognized for a similar application. As described in Section G.5, sufficient mixing to accomplish at least this reduction should occur on the basis of dispersion effects and the leakage volumes involved, and the most realistic model suggests that leakage would be conveyed upward by thermal currents to displace or mix with the air volume that is relieved through the filters during this expansion period.

Also, an arbitrary assumption of direct leakage with little or no mixing during this brief initial interval is regarded as an unrealistic and unnecessary extension of Safety Guide 4. Application of the conservative assumption of full instantaneous availability of fission product leakage to a secondary containment volume during this period would seem to warrant a reasonable mixing assumption consistent with the 100 percent instantaneous mixing that is assumed within the containment.

b. Filtered Release Before Recirculation Phase

The effectiveness of first-pass mixing during the first 20 minutes is less certain than that associated with recirculation, but use of a very conservative participation factor, such as 0.1, still obtains a factor of 3.1 for thyroid dose and 1.7 for the whole body dose, with deferred release of the annulus inventory considered and with decay neglected.

c. Recirculation of Halogens

A factor approximately equal on the minimum recirculation ratio is shown to apply to thyroid doses during recirculation, independent of mixing effects. The same factor has been recognized with regard to the standby gas treatment system for a BWR.

d. Recirculation of Noble Gas

Mixing of the recirculated flow in only twenty percent of the annulus volume is shown to obtain a reduction of six during the 20 minute to two hour period, with decay during holdup neglected and without credit for first pass mixing.

G.5 MIXING ANALYSIS AND POSSIBLE MIXING TESTS

Section G.5 describes analyses (including tables and figures) performed for the Final Safety Analysis Report. These analyses are strictly historical and have not been updated since the FSAR. No effort has been made to verify the information in this section. References to other sections of the safety analysis report within this section are applicable to the FSAR.

99064

The objectives of this section are:

1. to review the significance of mixing assumptions with regard to the total calculated dose.
2. to present an analysis of mixing effects that justifies the design assumptions.
3. to define the relevance of possible mixing tests and to consider their feasibility.

G.5.1 Significance of Mixing Assumptions in Dose Calculations

Section G.4 compared dose components associated with difference time intervals, with and without the attenuation caused by the Shield Building and its ventilation system (Columns 2 and 4 of Tables G.4-1 and G.4-2). Review of the factors of reduction applicable to these different dose components suggests the following order or importance to the aspects of Shield Building attenuation, insofar as they affect the total calculated dose.

- a. Thyroid dose reduction during the recirculation phase.
- b. Thyroid dose reduction during the 4.5 minute period of positive pressure.
- c. Whole body dose reduction during the 20 minute to 2 hour recirculation phase.
- d. Whole body dose reduction during the first 20 minutes of filters release.

As was shown in Section G.4.2, the first item is essentially independent of mixing assumptions for either the first or subsequent passes, because a large reduction factor occurs simply as a consequence of recirculation filtration. Substantiation of mixing would only serve to justify a calculated dose reduction of 30 or more for this component, rather than 20.

The significance of mixing, therefore, applies primarily to the remaining items, and, specifically, to the following aspects of these items.

- a. mixing with regard to unfiltered outleakage across the Shield Building annulus during the positive pressure period.
- b. first pass mixing enroute to the SBVS inlet as it affects the 0 to 20 minute and the 20 minute to 2 hour whole body doses.
- c. recirculation mixing as it affects the 20 minute to 2 hour whole body dose

Mixing effects are analyzed and the relevance and feasibility of possible mixing tests are considered in turn for each of these aspects of Shield Building effectiveness.

G.5.2 Mixing During Positive Pressure Period

Analysis of the effects of mixing upon the activity that might escape unfiltered across the Shield Building during the initial positive pressure period is based on several models that involve both large leaks and distributed leaks.

- a. Analysis Based on Large Leaks

Significant to evaluation of large leaks are the actual volumes of air that would leak into or out of the annulus during the period of positive pressure. The expected outleakage can be estimated on the basis of calculated annulus pressure and the maximum design leakage vs. pressure:

Case	Positive Pressure Period	Outleakage	Expanded Inleakage**
Normal heat transfer	2.6 min.	160* ft ³	56 ft ³
100% greater heat transfer	4.8 min.	640* ft ³	103 ft ³
Dose calculation	4.5 min.	1400 ft ³	

* somewhat underestimated because pressure is computed using higher outleakage.

** normalized to 1%/day initial containment leakage.

If the outleakage volume is regarded as one or more regular volumes adjacent to potential leaks in the outer wall which collapse as they leak out during the positive pressure period, and if no direct transport of the inleakage activity occurred from large leaks on the other side, then the outleakage volumes would not be intersected if they did not initially span the annulus.

Consideration of the volume of a single hemisphere (262 ft³) that would span the annulus, or other shapes that might reasonably be associated with leakage areas such as the door perimeters, plus consideration of the improbability of having directly opposed inleakage and outleakage sites, leads to a general conclusion that little, if any, direct leakage of activity would be expected on the basis of this model.

A separate model can be applied to the inleakage alone, recognizing that containment pressure could indeed cause part of the leakage from a large leak to be transported rapidly across the annulus. Figure G.5-1 shows the results of calculation of flow distribution from a circular jet corresponding to 1 percent per day leakage of the contents of the containment, approximately at design conditions (about 9 cfm leakage before expansion, through a single circular hole of 0.218 inch diameter). In this case, average dilution factors are calculated across vertical cross sections of the cone of expansion defined in the figure, and this average dilution is found to be 100 to 1 at the midpoint of the annulus and 200 to 1 at the outer wall. The dispersion characteristics of the mixing jet are supported by experimental measurements.⁽¹⁾

These models are useful in describing the condition of a large leak on one side of the annulus and distributed smaller leaks on the other. The extreme case of large leaks being directly opposed is not considered, because this assumption, compounded with the assumption of full instantaneous availability of fission products, would be unnecessarily conservative.

b. Analysis Based on Distributed Leaks

A more realistic model would consider mixing of inleakage flow with the substantial convective flow that will occur up the inside of the annulus during this period.

It may reasonably be expected that this will result in an overall mixing effect in the annulus similar to that assumed in the reference dose calculations. However, a conservative approach would be to assume that only a portion of the annulus air engages in the thermal movement and that the containment leakage mixes only with this air volume. For example, a thermal circuit could be postulated to occur up the inner wall and down the outer wall. In this case, the dose reduction could be determined directly on the basis of the participation factor associated with the circulating air volume involved, and the dose reduction factors previously discussed for low participation factor in Section G.4.2a would apply directly.

⁽¹⁾ Albertson, M. L., Dai, Y. B., Jensen, R. A., and Rouse, Hunter, "Diffusion of Submerged Jets," Proceedings, ASCE, Vol. 74, No. 10, December, 1948, pp. 1157-1196.

However, the amount of convective flow, if any, that would occur down the outer wall during this period is questionable in that the general overall process is one of thermal expansion and relief of air out the discharge vent. The disposition of the rising air would be expected to be primarily one of displacement or partial mixing with the 7 percent of the annulus air that is relieved from the dome area and discharge directly through the filters during the 4.5 minute period. This is regarded as the most useful model for the positive pressure period.

To the extent that this latter model is accurate, no unfiltered leakage would occur, and any dose adjustment would instead be that of adverse mixing applied to the 0 to 4.5 minute or the 0 to 20 minute filtered dose. As was demonstrated in Section G.4, this filtered component of the dose is not critical to an evaluation of the reduction factors that might be applied to the dual containment.

99064

c. No Meaningful Mixing Test

There appears to be no meaningful test that would directly demonstrate the effect of mixing upon the activity that might escape unfiltered across the Shield Building annulus during the initial 4.5 minute period of positive pressure.

Any direct test of transport would involve arbitrarily severe conditions of proximity and character of leaks on either side of the annulus, and it would not include the thermal effects which would most influence the transport and mixing processes during this period of an accident.

d. Improbability of Direct Release of Activity

However difficult it is to conservatively define mixing during this period, it may be noted that a far more difficult problem to prove, and perhaps an easier one to disprove, is the possibility that any measurable unfiltered activity could escape during this period - considering actual time of meltdown and transport and the effects of mixing on both sides of the containment shell, rather than applying the accepted premise of full instantaneous release and mixing within the containment that is part of Safety Guide 4.

G.5.3 Mixing During First Pass to Recirculation Inlet

A review of the locations of the containment penetrations that could leak into the annulus show that these are all at least 100 ft. below the level of the inlet header. Thus leakage from the expected sources will have a transport path equal to approximately half the height of the annulus before entering the duct leading to the filter and to the discharge and recirculation paths.

The results of analysis described in the next section for the recirculated component should apply generally to first-pass mixing of leakage from containment penetrations at elevations near that of the return header, where mixing of the leakage will be promoted by the nozzle action. As may be noted from Table G.2-1, a major part of the leakage will be from penetrations in this area.

A meaningful test of first-pass mixing applicable to the recirculation period might be feasible as part of the possible test that will be discussed for the recirculated component.

G.5.4 Mixing of the Recirculated Component

The effectiveness of mixing in the dual containment is least questionable with regard to mixing of the recirculated component once recirculation is established. Specific design features provided to ensure mixing during this period include: separation of the suction and inlet system headers at extreme ends of the building; maximum separation of the inlet header from the containment vessel penetrations near the bottom of the vessel, which are the expected sources of leakage; and distribution of return flow through 14 nozzles in the return header which are equally spaced around the lower circumference of the annulus to promote mixing of the containment leakage in the vicinity of the penetrations.

a. Mixing Analysis

The effectiveness of the nozzle distribution is indicated by the results of calculation described in Figure G.5-2, where centerline values are compared to those of relevant experiments. The nozzles are directed both upward and downward, and the calculation indicates that the expansion cone defined by 10 percent concentration limits relative to the header concentration would span the five foot annulus at a point 10 feet distant from the header.

The calculation demonstrates that substantial mixing will occur in the lower region of the annulus where leakage is expected, with first pass leakage being mixing with the return flow and with the volume of air in the lower part of the annulus. Also, velocities from the upward jets are dissipated rapidly with elevation, so channeling of the recirculated air flow should not occur for this reason.

b. Possible Mixing Tests

Recirculation mixing tests are not regarded as necessary to the evaluation because: 1) reasonable mixing is expected during this period; 2) the results would have significant application only to the 20 minute to 2 hour dose whole body dose; and 3) reasonable credit for mixing during this period appears justified on the basis of the previous discussion and the analysis of Section G.4.

Nevertheless, consideration has been given to the feasibility of such tests in response to specific suggestions by the Commission. As a result of this investigation, it is recognized that a meaningful cold mixing test applicable to the recirculation phase may be feasible because the thermal effects associated with the earlier phases of the accident will then have greatly diminished. The containment shell temperature at 20 minutes, for example, is predicted to be 200°F and the annulus air temperature has then risen to 160-180°F. Thus the temperature differences and the convective effects occurring during the cold test might not differ significantly from those of the 20 minutes to 2 hour accident period.

A possible mixing test would begin at equilibrium recirculation conditions, and a test of recirculation mixing would involve injection of a tracer substance into the return leg of the Shield Building ventilation system, with consequent entry into the annulus through the nozzles of the lower distribution header.

Two types of test might be considered: continuous injection and pulse injection.

With continuous injection of a substance that is not removable by filters, the concentration in the exhaust or recirculation flow should accumulate as shown in Table G.4.4 for noble gas without decay.

$$\left[1 - e^{-RP_0 t/f}\right] \approx RP_0 t/f$$

and the fraction of input discharge in time t should be:

$$\left[1 - \frac{1 - e^{-RP_0 t}}{RP_0 t}\right] = \left[\frac{RP_0 t}{2!} - \frac{(RP_0 t)^2}{3!} + \dots\right] = \frac{RP_0 t}{2f}$$

where RP_0 = discharge flow/total annulus volume
 f = participation fraction
 and other terms are as shown in Table G.4-4.

The fact that the Shield Building attenuation without filtration involves a large annulus capacitance, based on discharge flow rather than recirculation flow, thus permits a participation factor to be inferred directly from either the discharge concentration or the time-integrated discharge fraction. The fraction discharged in 100 minutes at 200 cfm discharge, 4000 cfm recirculation, and $f = 0.5$, for example, is only .052, so the accumulation is nearly linear, and both measurements are inversely proportional to an effective participation factor. The integrated discharge is simply .026/ f units per unit of total input.

A more useful result would be that from pulse injection with subsequent measurement of the transient concentration arriving at the discharge, or at any other point in the ducting beyond the inlet header. In this case, a discrete transport lag will occur in the first pass through the annulus before any tracer arrives, and the measured transient function represents a continuous distribution of all effects of transport delay, mixing and channeling associated with the different transport paths through the annulus.

In principle, this function could be applied directly to successive passes through the annulus to permit calculation of dose or dose reduction factors directly from the result of the experiment - independent of the concept of a participation factor. Similarly, a first pass transient function could be obtained by pulse injection at any point in the annulus, rather than in the return leg, and this result could similarly be included in the resulting dose analysis.

The possible direct use of the measured function can be demonstrated for the simple case designated as the actual flow pattern in Table G.4-4.

If we inject a brief pulse $S\Delta\tau$ of material in the return leg, and there exists full mixing in the annulus, tracer material will begin arriving immediately at the outlet of the annulus as:

$$PA_2 = SPe^{-PT} \Delta T$$

and the total amount that will be delivered is:

$$\int_0^{\infty} PA_2(T) dT = S$$

More generally, for an arrival function $G(T)$:

$$PA_2(T) = SPG(T)\Delta T$$

where

$$\int_0^{\infty} G(T) dT = I/P$$

By assuming full mixing in the ductwork at the completion of each pass, no time delay in the ductwork, and a fraction $1-R$ recirculated on each pass (as in Table G.4-4), the effects of repeated application of the measured function can be described.

The presence of a continuous source S during the last pass results in an outflow at time t:

$$PA_2(t) = PS \int_0^t G(t - T_1) dT_1$$

where the function G would be replaced with some other measured first-pass function in this expression if it were available (as would the last integrand in the subsequent equations that relate to previous passes).

At each time t-T, there existed an incoming recirculated flow associated with duration of the source during the previous pass, and this also contributes an outflow at time t:

$$PA_2(t) = P^2 S (I - R) \int_0^t G(t - T_1) \int_0^{T_1} G(T_1 - T_2) dT_2 dT_1$$

The total activity outflow is determined by extending this process to all previous passes and adding all contributions. The value of each multiple integral can be found from the use of the Laplace transform, where

$$L \{G(T)\} = g(\Delta)$$

and the summation is found to be:

$$\begin{aligned} L\{PA_2\} &= PS \left[\frac{g(\Delta)}{\Delta} + \frac{(I - R)Pg^2(\Delta)}{\Delta} + \frac{(I - R)^2 P^2 g^3(\Delta)}{\Delta} + \dots \right] \\ &= PS \frac{g(\Delta)}{\Delta [I - (I - R)Pg(\Delta)]} \end{aligned}$$

Similarly, the transform of the activity discharged from time 0 to t is:

$$\begin{aligned} L\left\{\int_0^t A_3 dt\right\} &= L\left\{\int_0^t RPA_2(t) dt\right\} \\ &= RPS \frac{g(\Delta)}{\Delta_2 [I - (I - R)Pg(\Delta)]} \end{aligned}$$

The two following examples provide some insight regarding the significance of a participation factor.

With full mixing, but only in a volume fraction f , as used in the reference calculations, we find:

$$G(T) = \frac{1}{f} e^{-PT/f}$$

$$g(\Delta) = \frac{1}{f(\Delta + P/f)}$$

$$L\{A_3\} = \frac{SRP}{f\Delta^2(\Delta + RP/f)}$$

and the inverse transform gives the same result as in Table G.4-4.

$$A_3 = \left[St \left(1 - \frac{1 - e^{-RPT/f}}{RPT/f} \right) \right]$$

Similarly, with all flow assumed to be slug flow, but only through a volume fraction f , all pulse activity arrives as a pulse of area $1/P$, delayed by a transit time f/P :

$$G(T) = \frac{1}{P} S \left(T - \frac{f}{P} \right) \quad \text{WHERE} \quad \begin{aligned} S &= 1 \text{ for } T = f/P \\ &= 0 \text{ for } T = f/P \end{aligned}$$

$$g(\Delta) = \frac{e^{-f\Delta/P}}{P}$$

$$L(A_3) = \frac{RS}{\Delta^2 [e^{f\Delta/P} - (1-R)]}$$

and the inverse transform is obtained:

$$A_3 = St \left[1 - (1-R)^m \right] \text{ for } m = 1, 2, 3, \dots$$

$$m < (Pt/f) < m + 1$$

In the recirculation phase, $P_t = 1.07$ for 100 minutes (20 min - 2 hr). Thus the 100 minute dose reduction factor with full volume slug flow is that for between 1 and 2 passes, or equal to R . the case $f = 0.5$ is between 2 and 3 passes, and the reduction is then $R(2-R) = .0975$. Similarly, the factor increases to .23 at $f = 0.2$ and approaches unity, as expected, at lower participation factors.

The participation factor, as used in the reference calculations, is simply an assumed reduction of capacitance to allow for the effects of nonuniformity in the mixing and transport process. The previous development and examples also suggest a physical interpretation of the factor as applied during recirculation. The convolution of a measured arrival concentration function effectively describes the behavior of particles which are confronted on each pass with a choice of transport paths through the full annulus, with each path characterized by a transport and mixing process. In contrast, the use of a participation factor is seen to represent a special case wherein a uniform process applies to all flow and where this uniform process is conservatively defined by assuming all flow to be directed through a reduced transit and mixing volume. The same process then applies uniformly during successive passes through the same volume fraction.

A more directly practical observation from the examples is that, even in the absence of mixing, slug flow through a reasonable fraction of the annulus volume would result in a reduction factor greater than the minimum credit proposed for the 20 minute to 2 hour whole body dose in Section G.4.3. Since this is the only dose component that would be significantly affected by the results of a mixing test, such a test is regarded as unnecessary.

G.6 SYSTEM TESTING

The system testing consists of the following:

G.6-1 Shield Building Ventilation System Testing.

The Shield Building Ventilation System Testing is described in Section 5.3.2. |

G.6-2 Auxiliary Building Special Ventilation System Testing.

The Auxiliary Building Special Ventilation System Testing is described in
Section 10.3.4. |

THIS PAGE IS LEFT INTENTIONALLY BLANK

PRAIRIE ISLAND UPDATED SAFETY ANALYSIS REPORT

USAR Appendix G
Revision 20

TABLE G.2-1 LEAKAGE PATHS INTO SHIELD BLDG. FROM CONTAINMENT

Penetration Number	Penetration Title	Nominal Line Size (inches)	Material	Testable
41A	Vacuum Breaker	18"	RG	Yes
41B	Vacuum Breaker	18"	RG	Yes
42A	Hydrogen Control	2"	MMS	Yes
42B	In Service Purge	18"	RG	Yes
43A	In Service Purge	18"	RG	Yes
50	Hydrogen Control	2"	MMS	Yes
	Equipment Hatch	252"	RG	Yes
	Personnel Airlock	80" (1)	RG	Yes
	Maintenance Airlock	80" (1)	RG	Yes
27B	Fire Protection	4"	RG	Yes
42C	Heating Steam	4"	RG	Yes
42F-1	Condensate Return	2"	RG	Yes
42F-2	Condensate Return	2"	RG	Yes
49B	Demin Water	2"	RG	Yes
19	Service Air	2"	RG	Yes

RG - Resilient Gasket

MMS - Metal to Metal Disk and Seat - less than 4" diameter

RG Total Diameter = 500"

MMS Total Diameter = 4"

(1) Largest dimension used

99177

99177

PRAIRIE ISLAND UPDATED SAFETY ANALYSIS REPORT

USAR Appendix G

Revision 34

**TABLE G.2-2 THROUGH LINE LEAKAGE THAT
BYPASS ANNULUS AND TERMINATES ABSVZ**

Penetration Number	Penetration Title	Nominal Line Size (inches)	Material	Testable
4	Vent Header	1"	RG	Yes
5	RCDT Pump Discharge	3"	RG	Yes
22	Cont Air Sample	1"	MMS	Yes
23	Cont Air Sample	1"	MMS	Yes
25A	Containment Purge	36"	RG	Yes
25B	Containment Purge	36"	RG	Yes
26	Sump Pump Discharge	3"	RG	Yes
27C-1	Cont Pressure Test Panel	1"	RG	Yes
27C-2	Cont Pressure Test Panel	1"	RG	Yes
35	Accumulator Test Line	3/4"	MMS	Yes
44	Cont Pressurization	6"	RG	Yes

RG - Resilient Gasket

RG Total Diameter = 87"

MMS - Metal to Metal Disk and Seat - valves less than 4" diameter MMS Total Diameter = 2.75"

01466114

PRAIRIE ISLAND UPDATED SAFETY ANALYSIS REPORT

USAR Appendix G
Revision 34

**TABLE G.2-3 THROUGH-LINE LEAKAGE THAT
BYPASSES BOTH ANNULUS AND ABSVZ**

Penetration Number	Penetration Title	Nominal Line Size (inches)	Material	Testable
1	PRT Sample	0.375"	MMS	Yes
2	PRT Nitrogen	0.750	RG	Yes
15	Sample	0.375"	MMS	Yes
16	Sample	0.375"	MMS	Yes
17	Sample	0.375"	MMS	Yes
18	Fuel Transfer	20	RG	Yes
20	Instrument Air	2	MMS	Yes
21	RCDT to Gas Analyzer	0.375"	MMS	Yes
31	Accumulator Nitrogen	1	MMS	Yes
42A	Hydrogen Control	2"	MMS	Yes
45	Water to PRT	2	MMS	Yes
50	Hydrogen Control	2"	MMS	Yes

RG - Resilient Gasket

MMS - Metal to Metal Disk and Seat - valves less than 4" diameter

RG Total Diameter = 20.75"

MMS Total Diameter = 10.875"

01466114

PRAIRIE ISLAND UPDATED SAFETY ANALYSIS REPORT

USAR Appendix G
Revision 4

**TABLE G.3-1 CALCULATIONAL BASES FOR SHIELD BUILDING
MAXIMUM INTERNAL PRESSURE POST DBA**

Category	Input	Remark
Initial Conditions and Boundary Conditions	Annulus pressure	14.79 psia Includes 0.09 psia due to shell expansion
	Ambient pressure	14.7 psia
	Annulus temperature	120°F
	Concrete temperature	120°F
Properties	Ambient temperature	120°F
	Air density	0.068 lb/ft ³ (at 120°F) Varies from 0.073 lb/ft ³ to 0.062 lb/ft ³ at 70°F and 160°F respectively
	Steel density	490 lb/ft ³
	Concrete density	144 lb/ft ³
	Air heat density	0.24 Btu/lb°F
	Steel heat density	0.115 Btu/lb°F
	Concrete heat capacity	0.2 Btu/lb°F
	Air conductivity	0.019 Btu/hr-ft°F
	Steel conductivity	26 Btu/hr-ft°F
	Conductivity	0.8 Btu/hr-ft°F
	Air viscosity	0.0474 lb/ft-hr Varies from 0.0441 lb/ft-hr to 0.0491 lb/ft-hr at 70°F and 160°F respectively
	Air Prandtl Number	0.71

TABLE G.3-2 SUMMARY OF PARAMETER STUDY

Figure	No. of SBVS	Heat Transfer Coefficient (see Note-1 Below)	Shield Bldg Leak Rate	Parameter Shown on Figure
G.3-1	NA	25% over Tagami (See Note 2)	NA	Reactor Containment Vessel Dome and Cylindrical Wall Outside Surface Temperature.
G.3-2 & G.3-3	NA	NA	NA	Flow Paths for the SBVS.
G.3-4	1	Normal	Normal	Annulus Air Temperature.
G.3-5 & G.3-6	2	Normal	Normal	Pressure and Flow.
G.3-7 & G.3-8	1	-33%	Normal	Pressure and Flow.
G.3-9 & G.3-10	1	+25%	Normal	Pressure and Flow.
G.3-11 & G.3-12	1	Normal	Variable 10% to 100%	Pressure and Flow.
G.3-13 & G.3-14	1 1	Normal Normal	Normal Normal	Pressure and flow assuming concrete as an adiabatic wall.
G.3-15 & G.3-16	1	+25%	1% and 10%	Pressure and Flow.
G.3-17	NA	NA	NA	Wind 40 mph
G.3-18 & G.3-19	2	+25%	1% and 10%	Pressure and Flow.

Note1: Heat transfer Coefficient variation was made on the external surface of the Reactor Containment Vessel and involves varying the natural convection heat transfer coefficient from the steel shell to air in the annulus.

Note 2: The temperature of the Reactor Containment Vessel shell is obtained from the containment vessel pressure-temperature transient using a heat transfer coefficient to the containment internal surface that is 25% higher than that obtained from Tagami's work. This temperature is then used for all transient studies.

TABLE G.3-3 TWO-HOUR DOSE AT SITE BOUNDARY

Shield Building, 0.0089/day	Rem
0 ~ 7 minutes unfiltered leakage	4.05
0 ~ 20 minutes filtered leakage	6.29
20 min. ~ 2 hr. recirculation phase	<u>12.85</u>
Total Shield Building	23.19
Auxiliary Building, 0.001/day	53.00
Direct leakage, 0.0001/day	<u>53.00</u>
Total 2-hr. Dose	129.19

Containment leakage rate of 0.01/day, filter efficiency of 0.90 and shield participation of 0.50.

**TABLE G.3-4 SHIELD BUILDING DISCHARGE AND RECIRCULATION
FOLLOWING A LOSS-OF-COOLANT ACCIDENT**

Time	Direct Leak	Filtered Venting	Recirculation
0 ~ 36 sec	292%/day	0	0
36 sec ~ 7 min	292%/day	7000 cfm	0
7 ~ 12 min	0	2200 cfm	0
12 ~ 20 min	0	500 cfm	0
20 min ~ 1 day	0	200 cfm	5300 cfm
1 ~ 30 day	0	200 cfm	5300 cfm

PRAIRIE ISLAND UPDATED SAFETY ANALYSIS REPORT

USAR Appendix G
Revision 18

TABLE G.4-1 COMPARISON OF THYROID DOSE CALCULATIONS FOR NORMALIZED TOTAL CONTAINMENT LEAKAGE RATE OF .01/DAY, ALL DOSES IN REMS

	Column 1 Reference Case 95% Filter	Column 2 Reference Case Adjusted to 90% Filter	Column 3 Suggested Basis - 70% Direct Transport to 90% Filter	Column 4 Total Dose Potential Single Containment With 90% Filter
<u>Doses at Site Boundary</u>				
Shield Building, .0089/day				
0-4.5 minutes unfiltered leakage	0.64	0.64		184.62
0-20 minutes filtered release	2.70	6.04	56.02	62.97
20 min-2 hr recirculation release	<u>7.94</u>	<u>15.09</u>	<u>18.98</u>	<u>391.01</u>
Total Shield Bldg.	11.28	21.77	75.00	638.60
Aux. Bldg., .001/day	26.54	53.08	53.08	53.08
Direct Leakage, .0001/day	<u>53.08</u>	<u>53.08</u>	<u>53.08</u>	<u>53.08</u>
Total 2 hr dose	90.90	127.93	181.16	744.76
<u>Doses at Low Population Zone</u>				
0-2 hr Shield Bldg. only	2.84	5.47	18.81	160.13
0-30 days:				
Shield Bldg.	13.98	28.78	42.61	597.20
Aux. Bldg.	32.01	64.02	64.02	64.02
Direct Leakage	<u>64.02</u>	<u>64.02</u>	<u>64.02</u>	<u>64.02</u>
Total 0-30 days	110.01	156.82	170.65	725.24
<u>Doses Using Safety Guide 4 Meteorology Values Instead</u>				
0-2 hr, Site Boundary	96.53	135.83	192.30	790.59
0-3 days, LPZ	105.52	149.81	162.05	701.

99064

PRAIRIE ISLAND UPDATED SAFETY ANALYSIS REPORT

USAR Appendix G

Revision 18

TABLE G.4-2 COMPARISON OF WHOLE BODY DOSE CALCULATIONS FOR NORMALIZED TOTAL CONTAINMENT LEAKAGE RATE OF .01/DAY, ALL DOSES IN REMS

	Column 1 Reference Case 95% Filter	Column 2 Reference Case Adjusted to 90% Filter	Column 3 Suggested Basis - 70% Direct Transport to 90% Filter	Column 4 Total Dose Potential Single Containment With 90% Filter	
<u>Doses at Site Boundary</u>					
Shield Building, .0089/day					
0-4.5 minutes unfiltered leakage	.003	.003	.083	.039	
0-20 minutes filtered release	.174	.174	7.005	10.479	
20 min-2 hr recirculation release	<u>1.499</u>	<u>1.499</u>	<u>2.722</u>	<u>38.503</u>	
Total Shield Bldg.	1.676	1.676	9.810	49.021	
 Aux. Bldg., .001/day	5.518	5.518	5.518	5.518	
Direct Leakage, .0001/day	<u>.552</u>	<u>.552</u>	<u>.552</u>	<u>.552</u>	
Total 2 hr dose	7.746	7.746	15.88	55.091	
<u>Doses at Low Population Zone</u>					
0-2 hr Shield Bldg. only	.421	.421	2.460	12.316	
0-30 days:					
Shield Bldg.	4.442	4.442	7.059	33.820	
Aux. Bldg.	3.800	3.800	3.800	3.80	
Direct Leakage	<u>.380</u>	<u>.380</u>	<u>.380</u>	<u>.380</u>	
Total 0-30 days	8.622	8.622	11.239	38.000	
<u>Doses Using Safety Guide 4 Meteorology Values Instead</u>					
0-2 hr, Site Boundary	8.22	8.22	16.86	58.58	
0-3 days, LPZ	8.42	8.42	10.68	34.31	

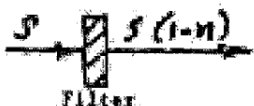
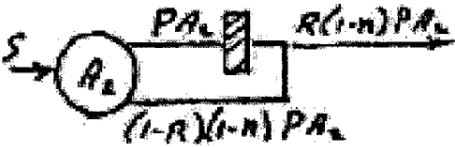

49066

PRAIRIE ISLAND UPDATED SAFETY ANALYSIS REPORT

USAR Appendix G

Revision 4

TABLE G.4-3 SIMPLIFIED REDUCTION FACTORS
FOR 20 MINUTE TO 2-HOUR THYROID DOSE




Case	Equations	Dose Reduction Factor = $A_3 / S(1-n)t$
<u>Direct Discharge</u> 	$\dot{A}_1 = S(1-n)$ $A_3 = S(1-n)t$	<div style="border: 1px solid black; padding: 5px; display: inline-block;"> <p>R = Recirculation ratio = 200 cfm/4000 cfm = .05</p> <p>Pt = 2.14 (100 minutes, 4000 cfm, and 0.1 participation factor)</p> </div> <div style="text-align: right; font-size: 2em; margin-top: 20px;">1</div>
<u>Actual Flow Pattern</u> 	$\dot{A}_2 = S + 0.4R(1-n)PA_2 - PA_2$ $= S - \alpha A_2$ <p>where $\alpha = P[1 - 0.4R(1-n)]$</p> $A_2 = \frac{S}{\alpha}(1 - e^{-\alpha t})$ $\dot{A}_3 = (1-n)RPA_2$	$\frac{RP}{\alpha} \left[1 - \frac{1 - e^{-\alpha t}}{\alpha t} \right]$ $= \frac{A_3}{S} (.567) \text{ for } n = .95$ $= \frac{A_3}{S} (.562) \text{ for } n = .90$ $= \frac{.915}{.051} \text{ for Boru}$ $\approx \frac{.915}{.051} \left[1 - \frac{1 - e^{-\alpha t}}{\alpha t} \right]$
<u>No Plant Free Mixing</u> 	$\dot{A}_3 = (1-n)(1-R)(S+PA_2) - PA_2$ $= S(1-n)(1-R) - \alpha A_2$ <p>where α is defined above</p> $A_2 = \frac{S(1-n)(1-R)}{\alpha}(1 - e^{-\alpha t})$ $\dot{A}_3 = R(1-n)(S+PA_2)$	$R \left\{ 1 + \frac{0.4R(1-n)P}{\alpha} \left[1 - \frac{1 - e^{-\alpha t}}{\alpha t} \right] \right\}$ $= R \left\{ 1 + .051 \left[1 - \frac{1 - e^{-\alpha t}}{\alpha t} \right] \right\}$ $= .051 \text{ for } n = .95$ $= R \left\{ 1 + .109 \left[1 - \frac{1 - e^{-\alpha t}}{\alpha t} \right] \right\}$ $= .053 \text{ for } n = .90$

PRAIRIE ISLAND UPDATED SAFETY ANALYSIS REPORT

USAR Appendix G

Revision 4

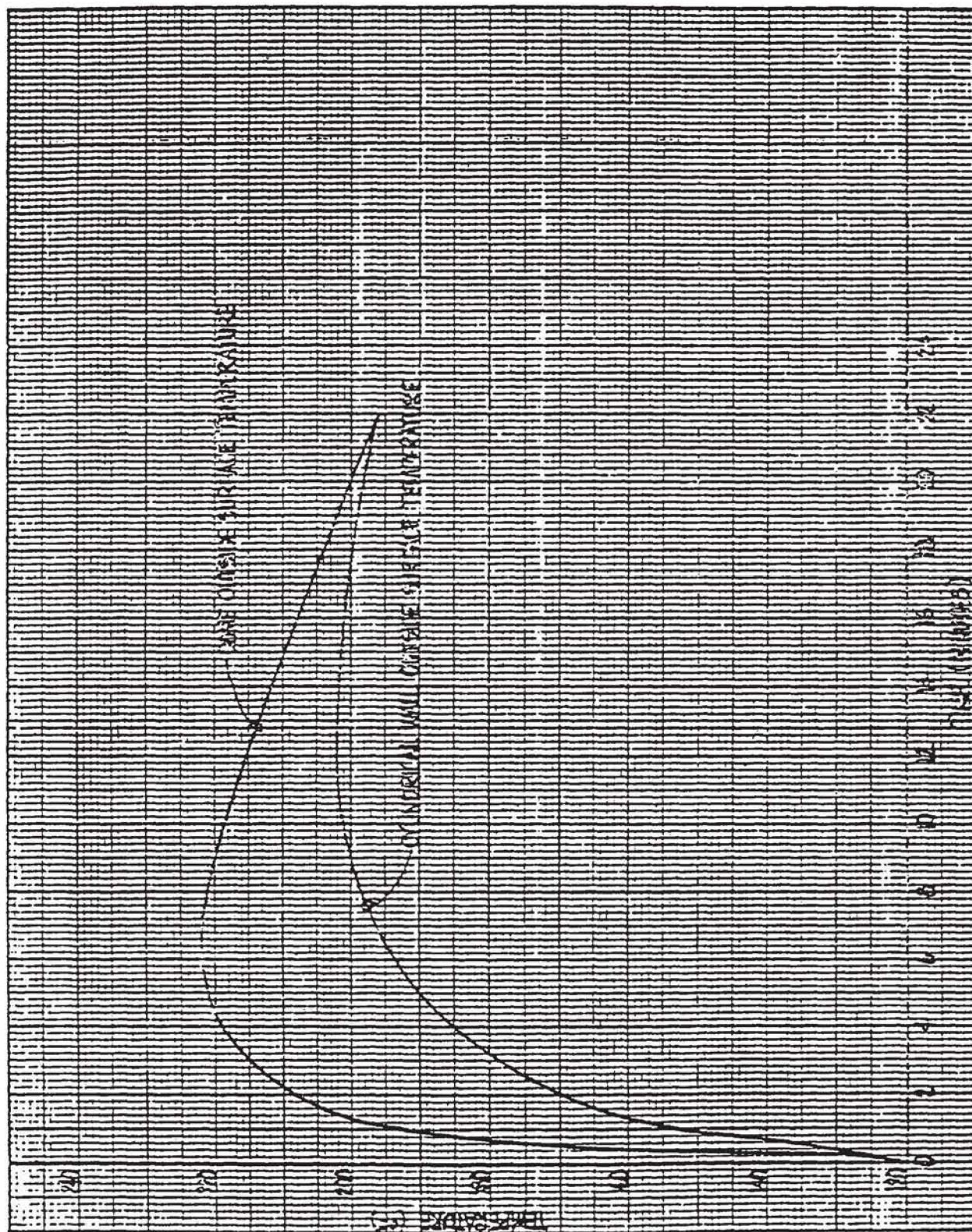
TABLE G.4-4 SIMPLIFIED REDUCTION FACTORS
FPR 20 MINUTE TO 2 HOUR WHOLE BODY DOSE

Case	Equations	Dose Reduction Factor = A_3 / S_0
<u>Direct Discharge</u> 	$\dot{A}_1 = S$ $A_3 = S t$	<div style="border: 1px solid black; padding: 5px; display: inline-block;"> $R = \text{Recirculation ratio}$ $= 200 \text{ cfm} / 4000 \text{ cfm} = .05$ $P_L = 2.14$ (100 minutes, 4000 cfm, and 0.5 participation factor) </div> <div style="text-align: right; font-size: 2em;">1</div>
<u>Actual Flow Pattern</u> 	$\dot{A}_1 = S - RPA_2$ $A_2 = \frac{S}{RP} (1 - e^{-RPe})$ $\dot{A}_3 = RPA_2$	$\left[1 - \frac{1 - e^{-RPe}}{RPe} \right]$ $= \underline{\underline{.0517}}$
<u>No First Pass Mixing</u> 	$\dot{A}_1 = (1-R)S - RPA_2$ $A_2 = \frac{(1-R)S}{RP} (1 - e^{-RPe})$ $\dot{A}_3 = R(S + PA_2)$	$R + (1-R) \left[1 - \frac{1 - e^{-RPe}}{RPe} \right]$ $= .05 + .95 (.0517)$ $= \underline{\underline{.099}}$

**TABLE G.4-5 SHIELD BUILDING DISCHARGE AND RECIRCULATION
FOLLOWING A LOSS-OF-COOLANT ACCIDENT**

Time Period	Direct Leakage	Filtered Venting	Recirculation
0-36 seconds	120 per day*	0	0
36 sec-4.5 mins	120 per day*	6000 cfm	0
4.5-10 minutes	0	3000 cfm	0
10-20 minutes	0	820 cfm	0
20 mins-1 day	0	200 cfm (77% per day)*	4000 cfm
1 day - 30 days	0	200 cfm (77% per day)*	4000 cfm

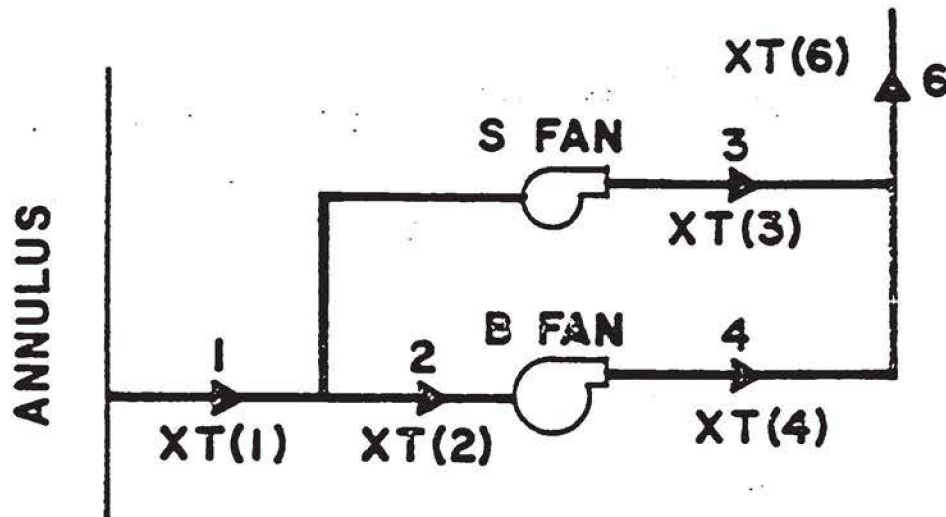
* Percent per day of the shield building or annulus volume



CONTAINMENT DOME & CYLINDRICAL WALL OUTSIDE
SURFACE TEMPERATURE TRANSIENT.

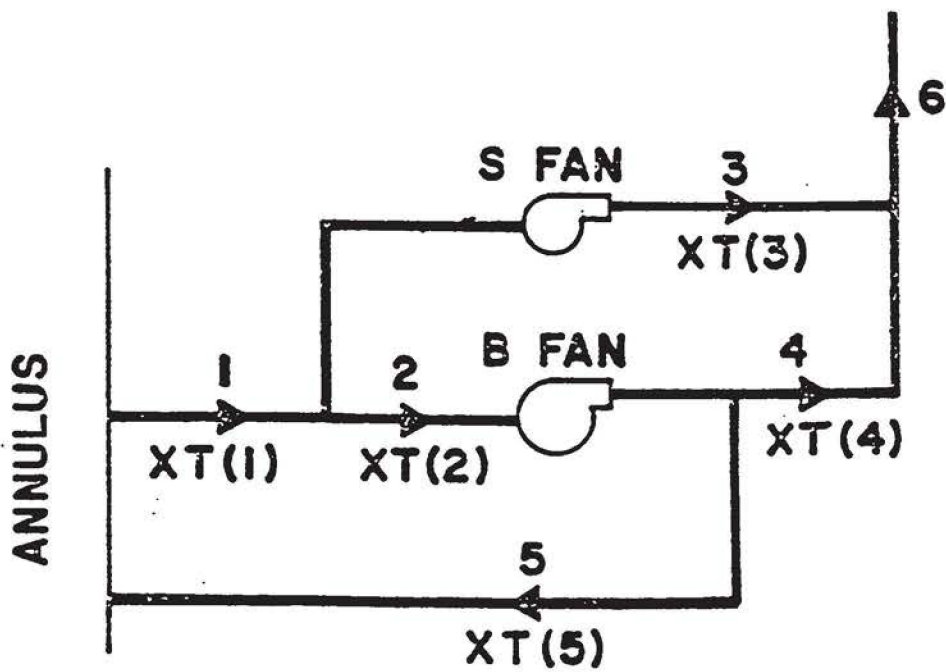
FIGURE G.3-1

REV 4 12/85



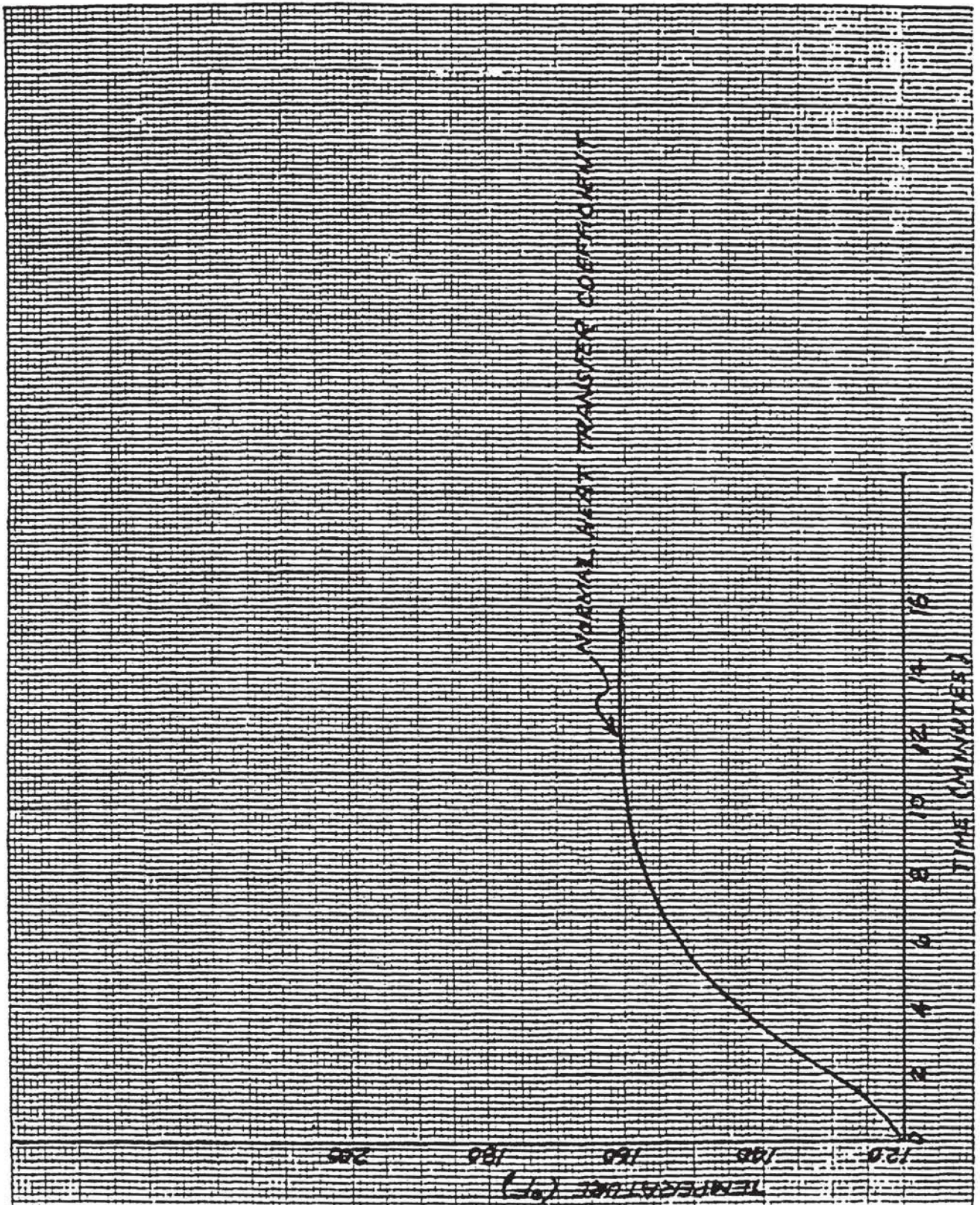
CONFIGURATION WITHOUT RECIRCULATION

FIGURE G.3-2



CONFIGURATION WITH RECIRCULATION

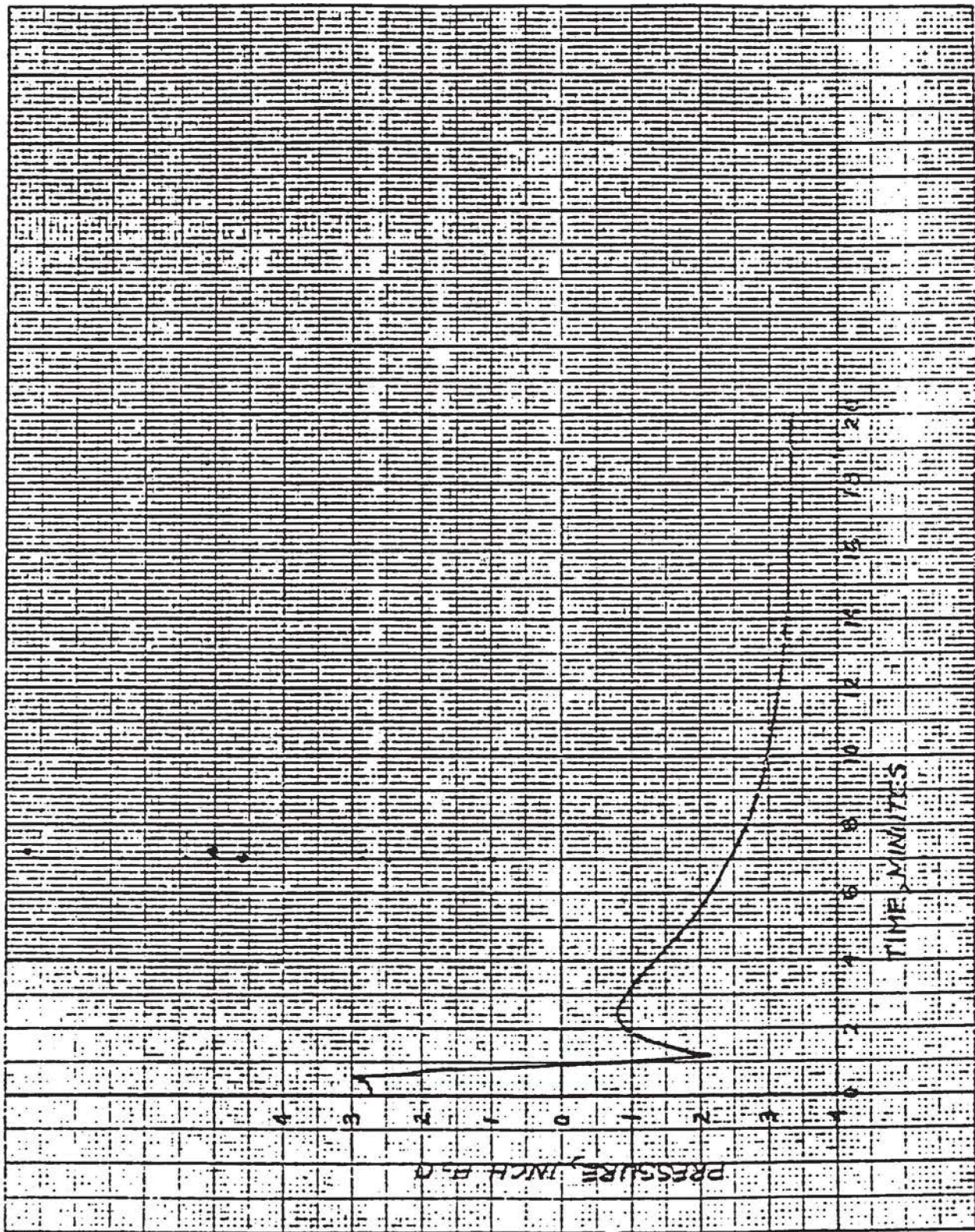
FIGURE G.3-3



ANNULUS AIR TEMPERATURE

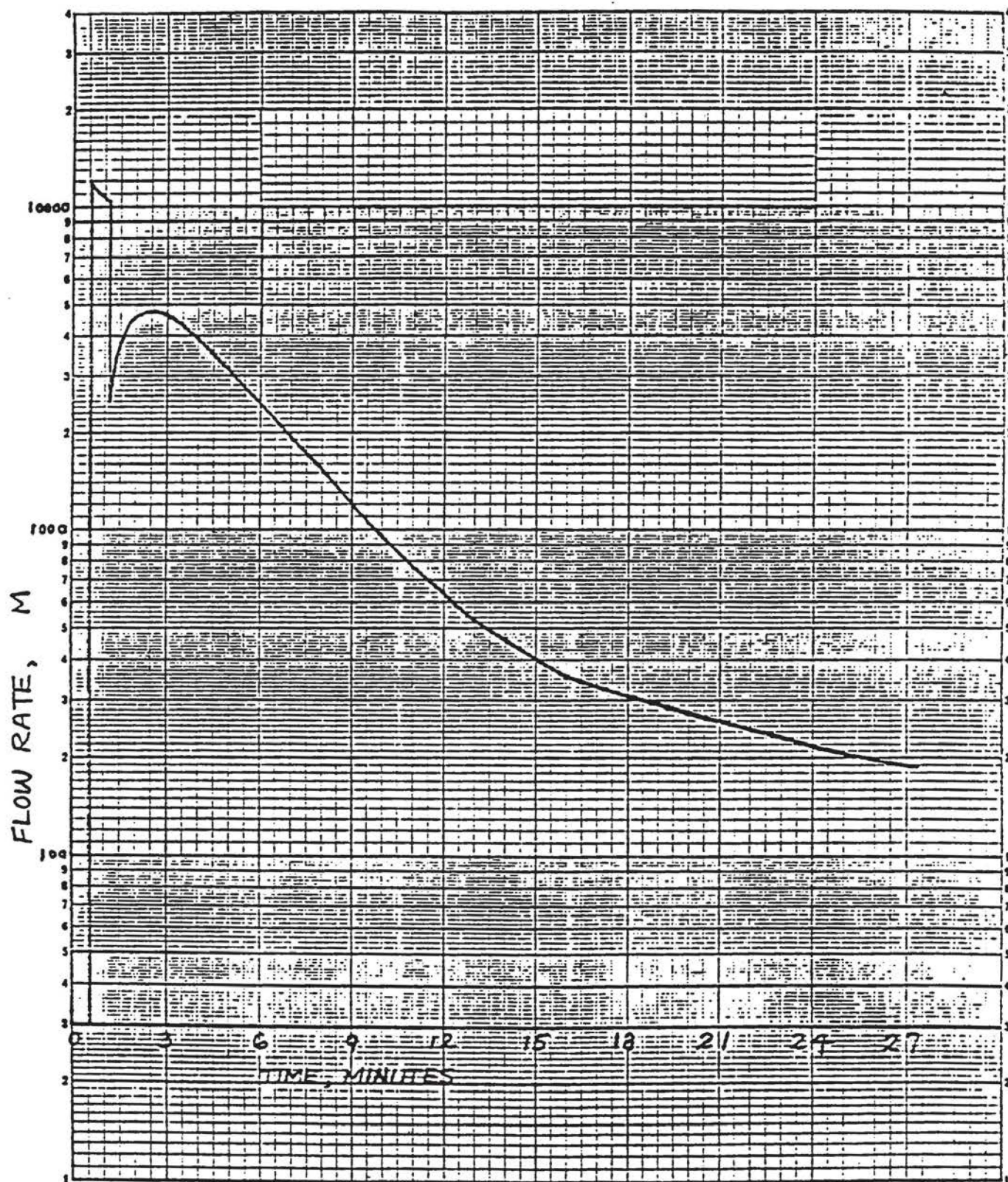
FIGURE G.3-4

REV 4 12/8



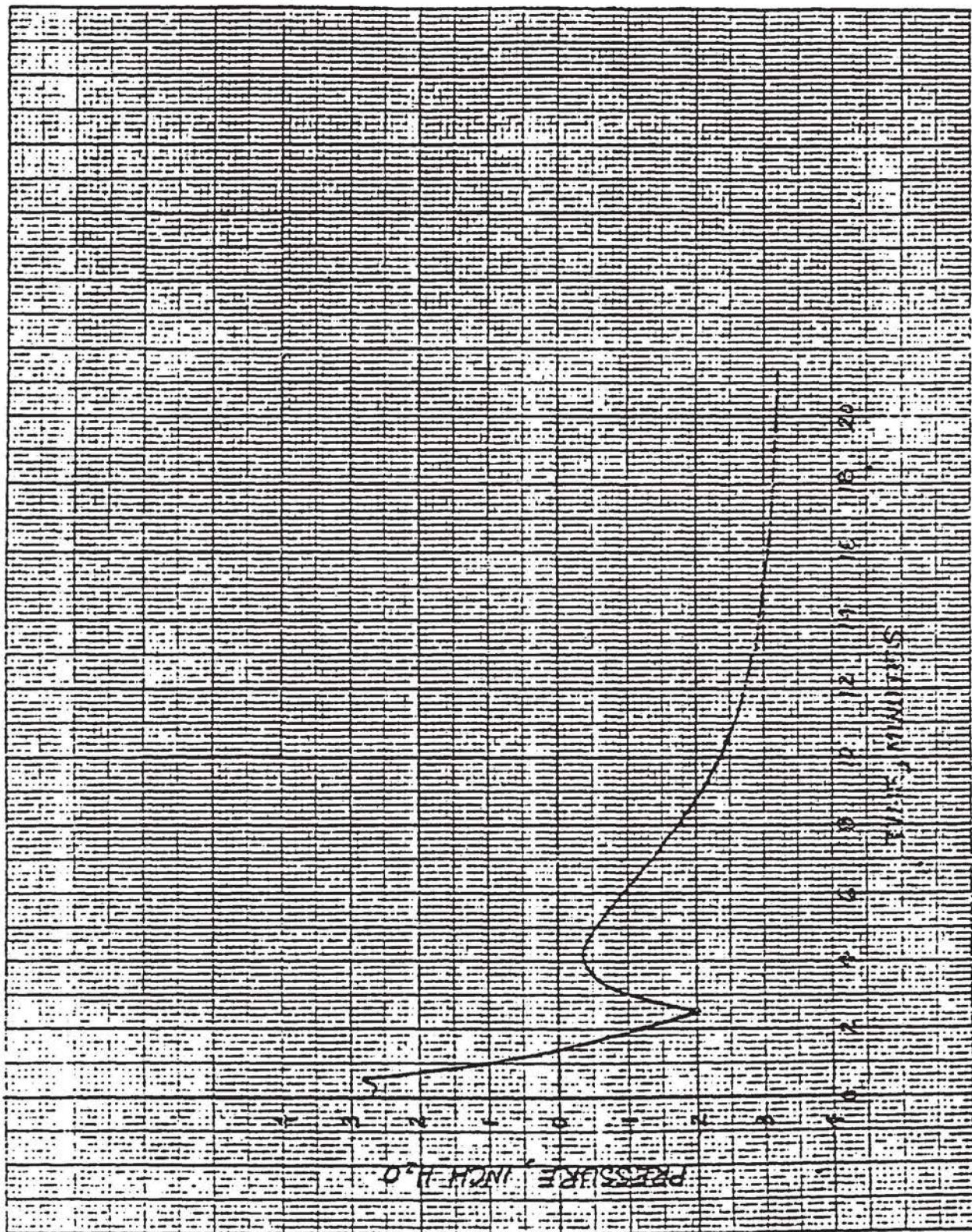
ANNULUS PRESSURE
(Both SBVS Operating)

FIGURE G.3-5



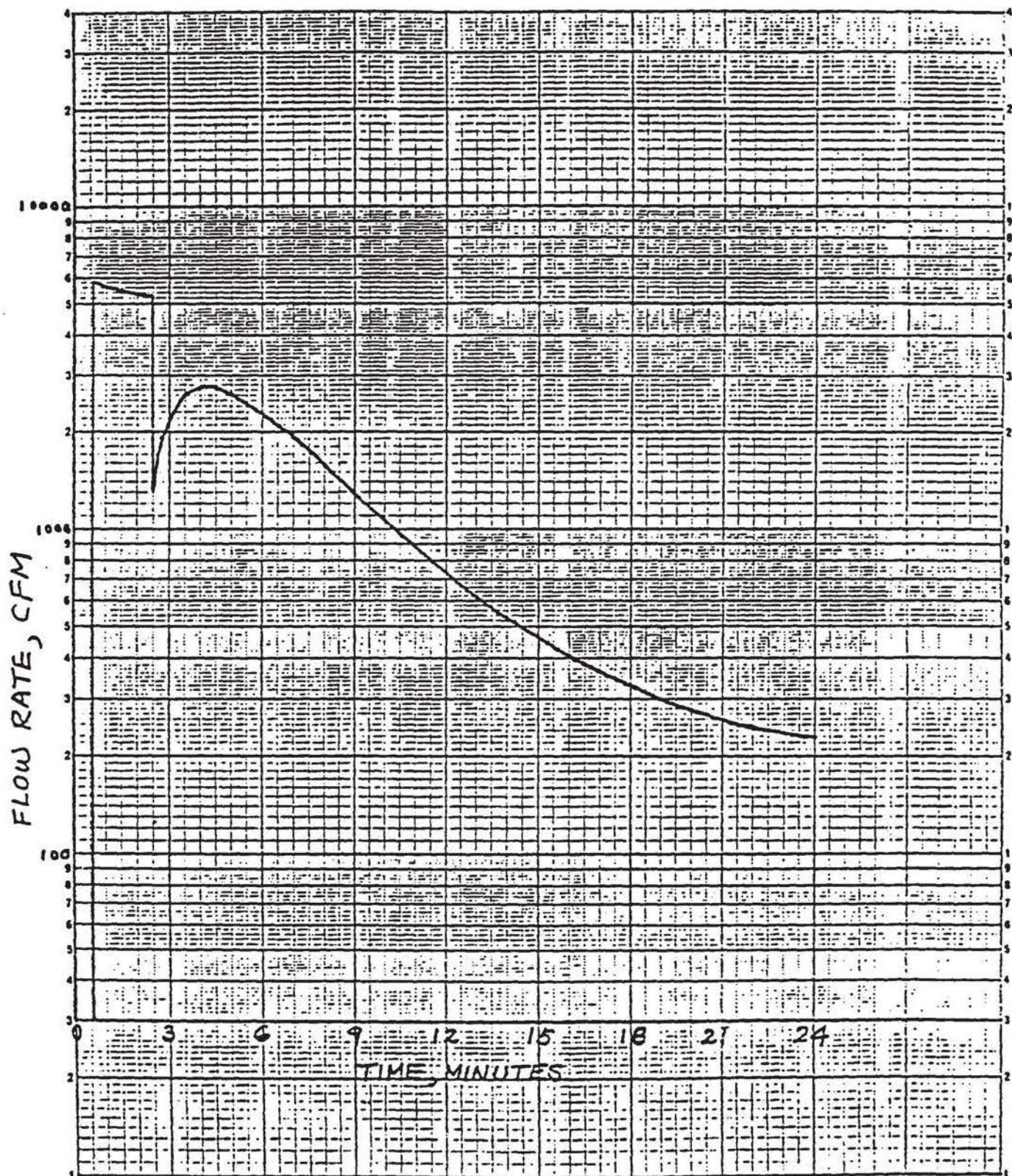
FLOW OUT OF SBVS
(Both SBVS Operating)

FIGURE G.3-6



ANNULUS PRESSURE
(33% Lower H.T. Coeff.)

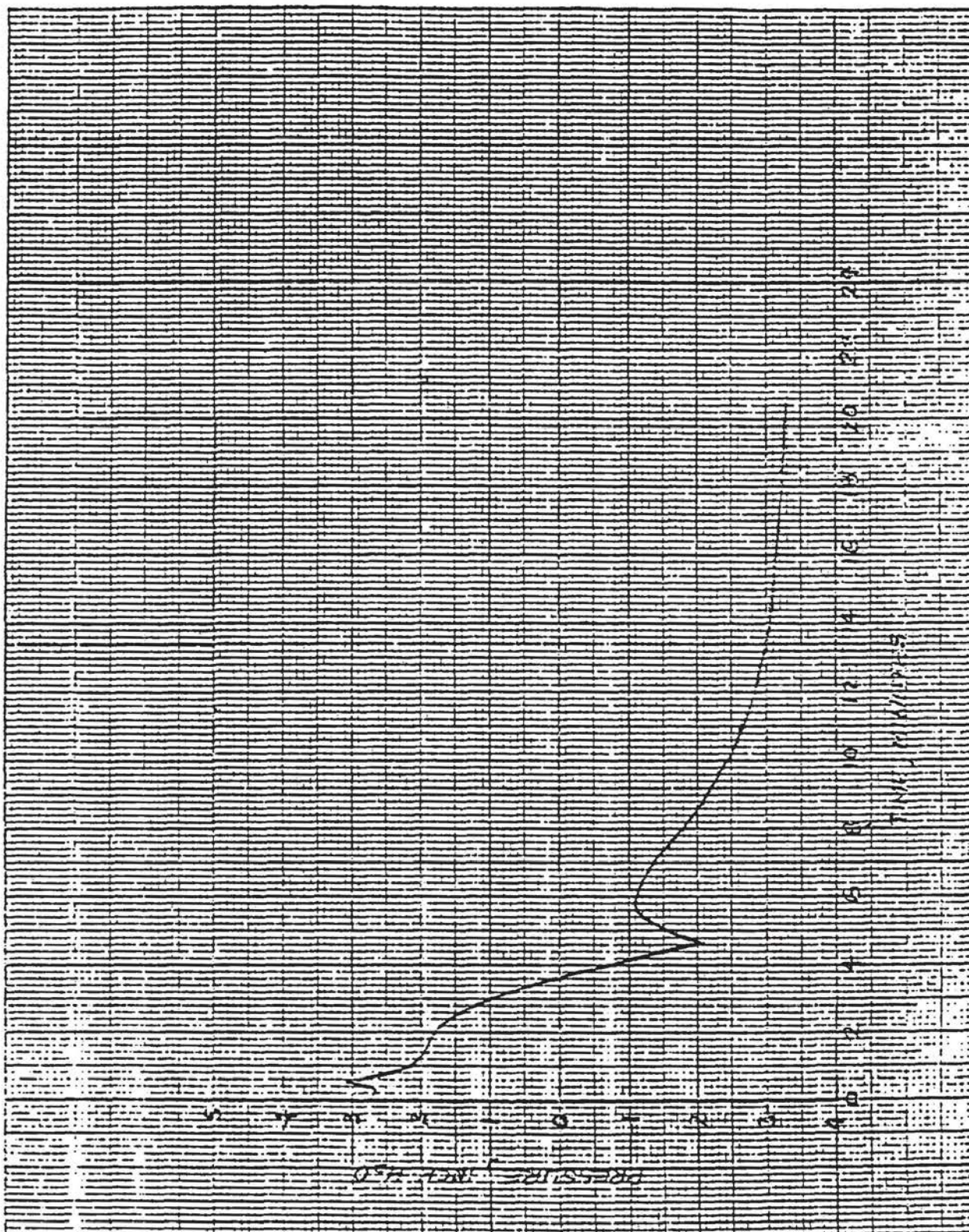
FIGURE G.3-7



FLOW OUT OF SBVS (33% LOWER H.T. Coeff)

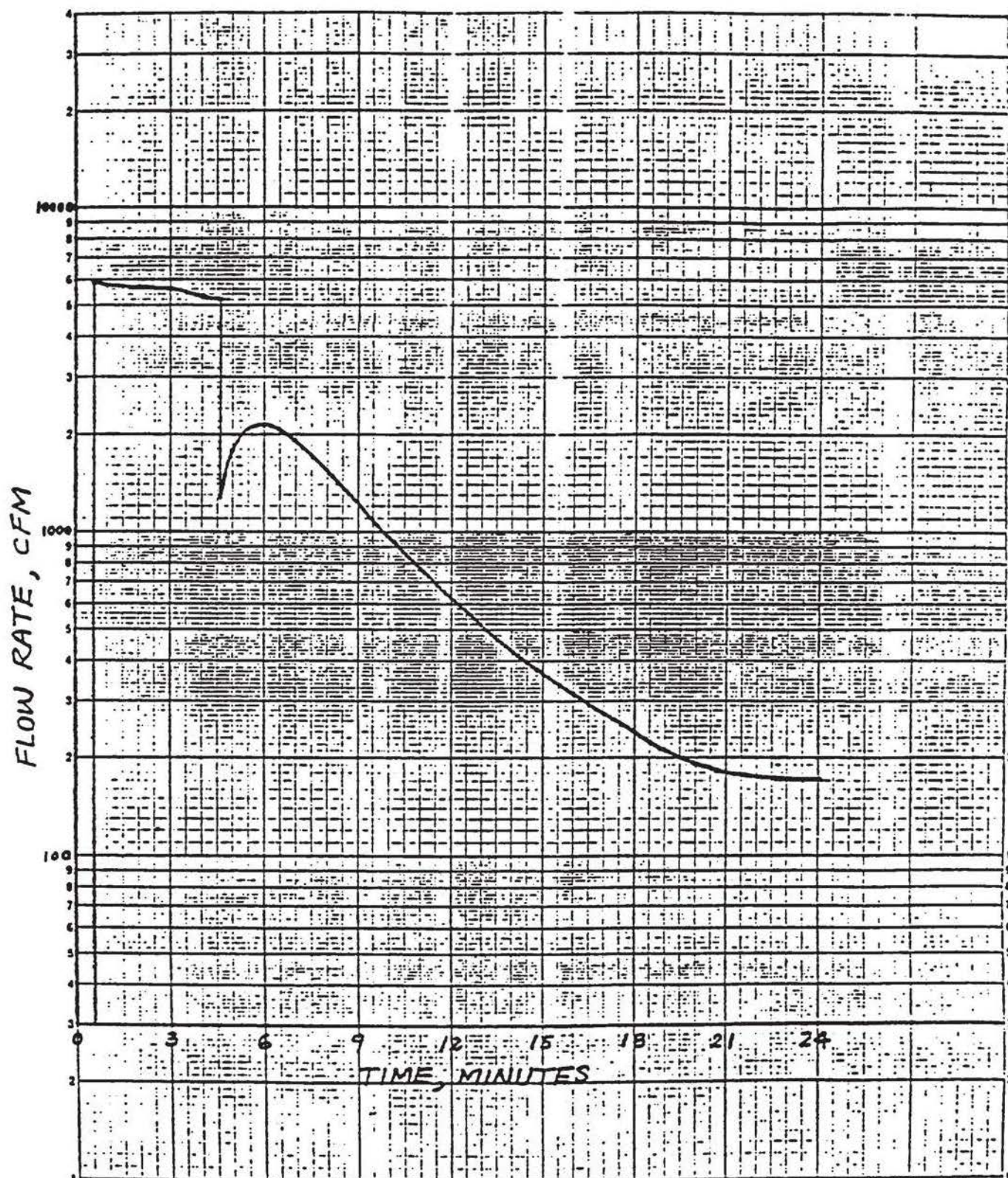
FIGURE C.3-8

REV 4 12/85



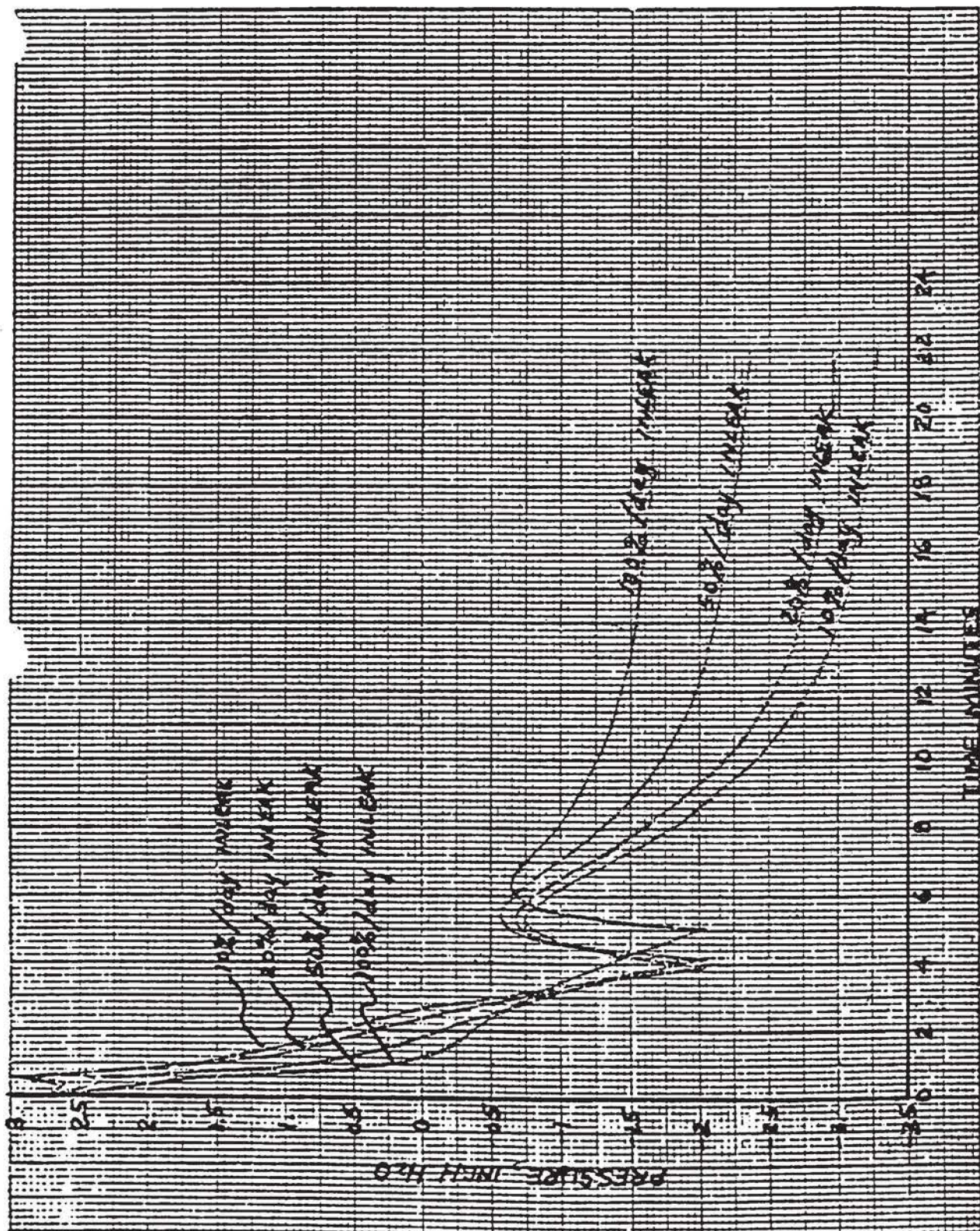
ANNULUS PRESSURE
(25% Higher H.T. Coeff.)

FIGURE G.3-9



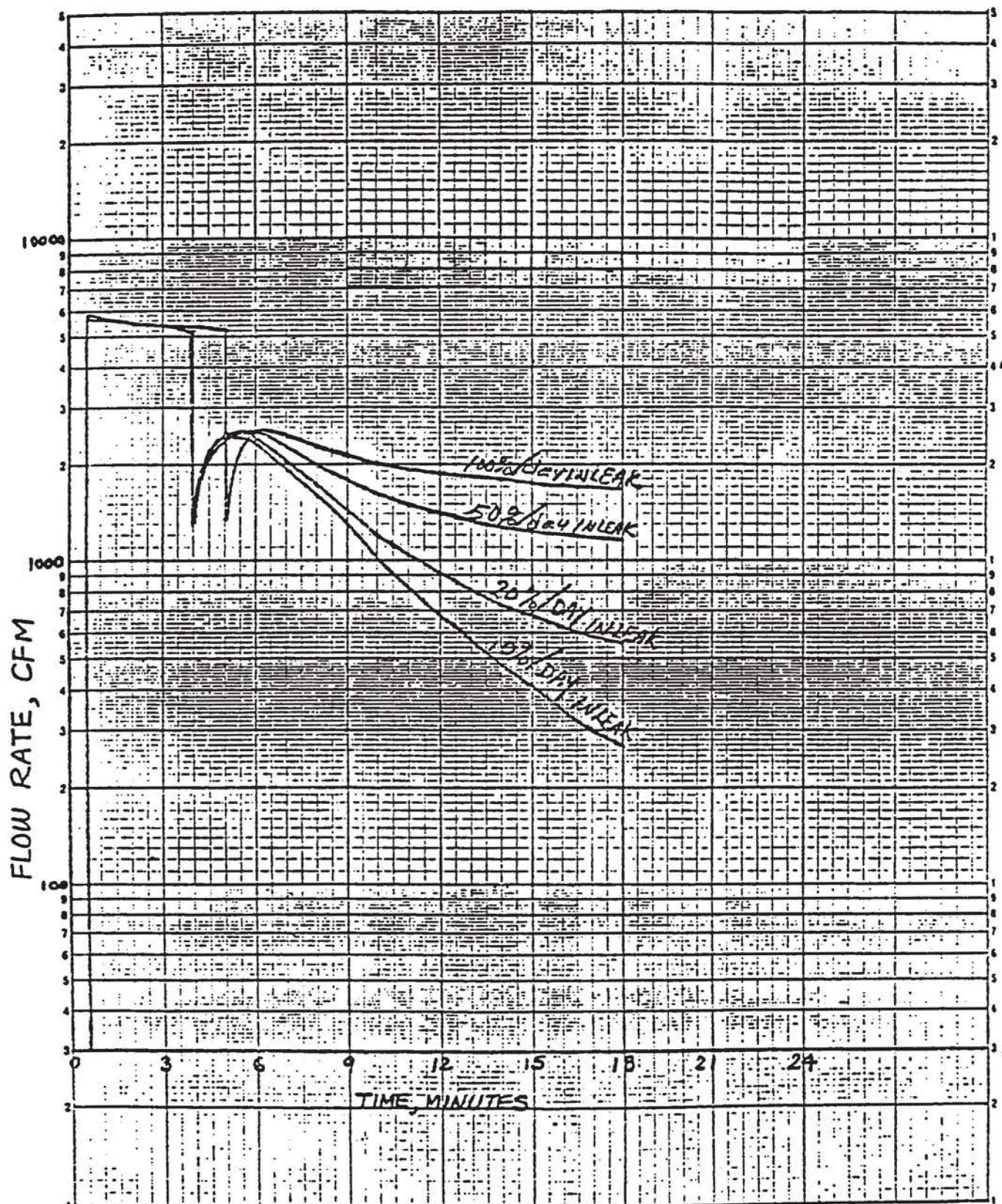
FLOW OUT OF SBVS
(25% Higher H.T. Coeff.)

FIGURE G.3-10



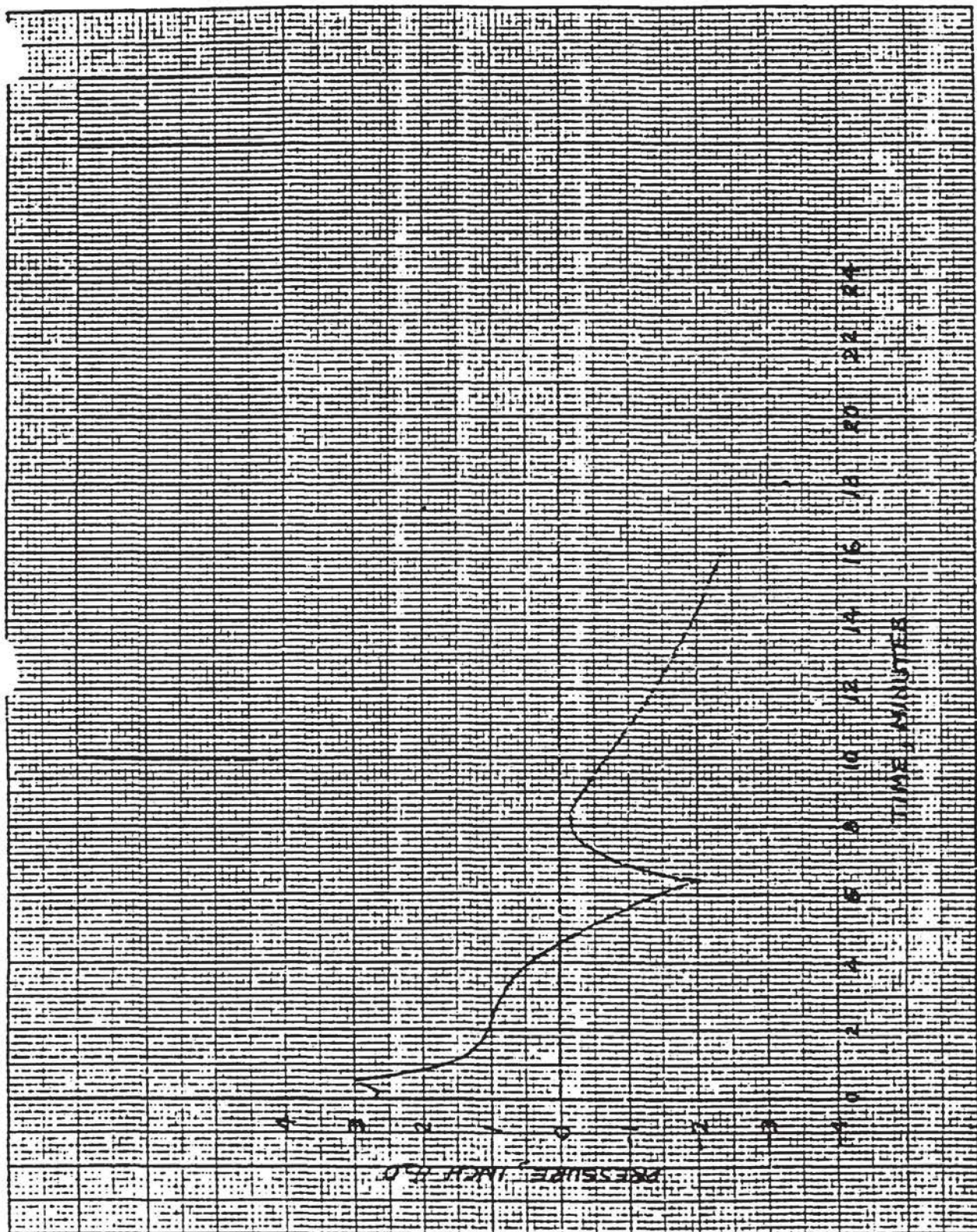
ANNULUS PRESSURE (SHIELD BUILDING LEAKAGE)

FIGURE G.3-11



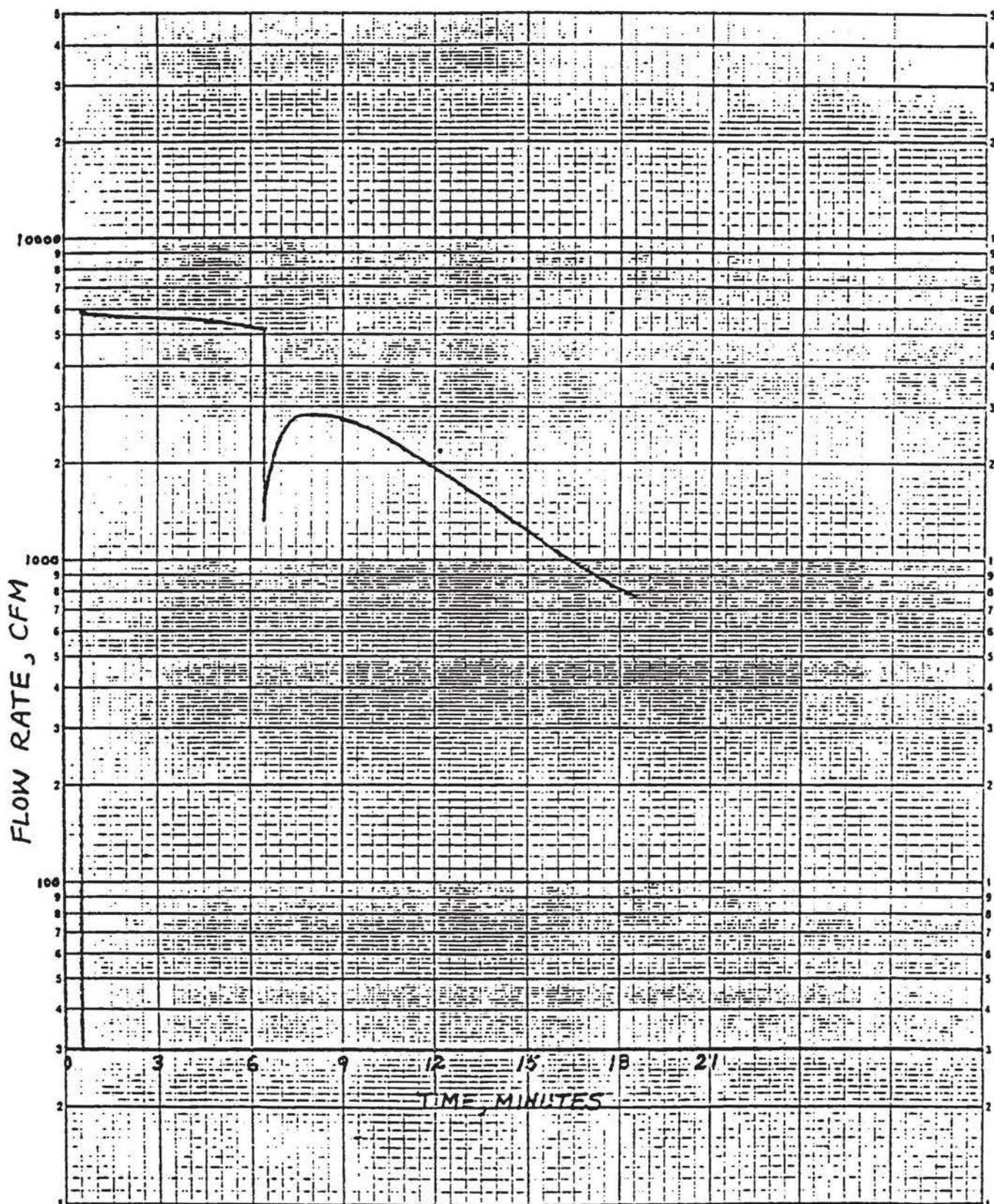
FLOW OUT OF SBVS (SHIELD BUILDING LEAKAGE)

FIGURE G.3-12



ANNULUS PRESSURE
WITHOUT HEAT TRANSFER TO CONCRETE WALL

FIGURE G.3-13



FLOW OUT OF SBVS
WITHOUT HEAT TRANSFER TO CONCRETE WALL

FIGURE G.3-14

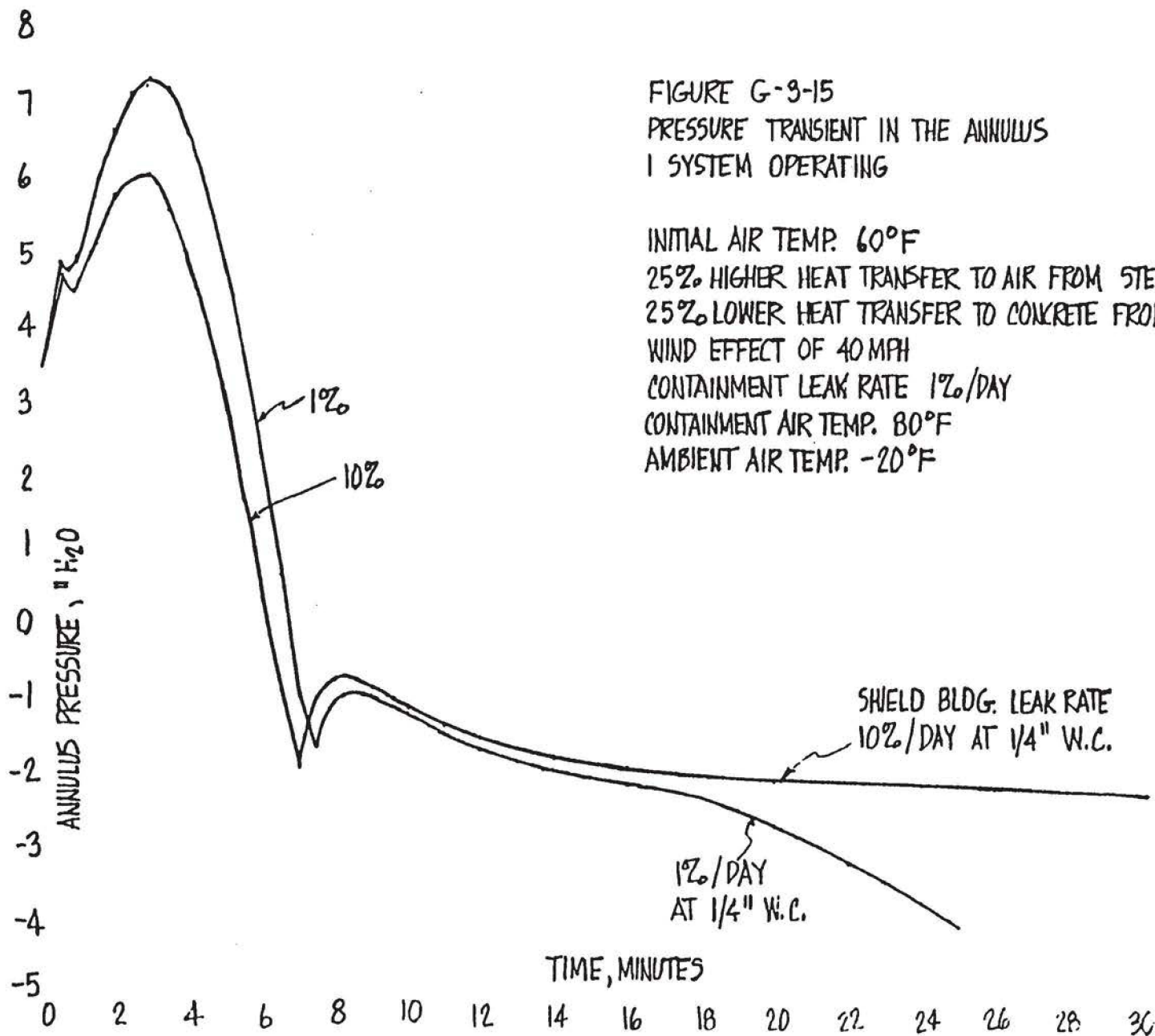
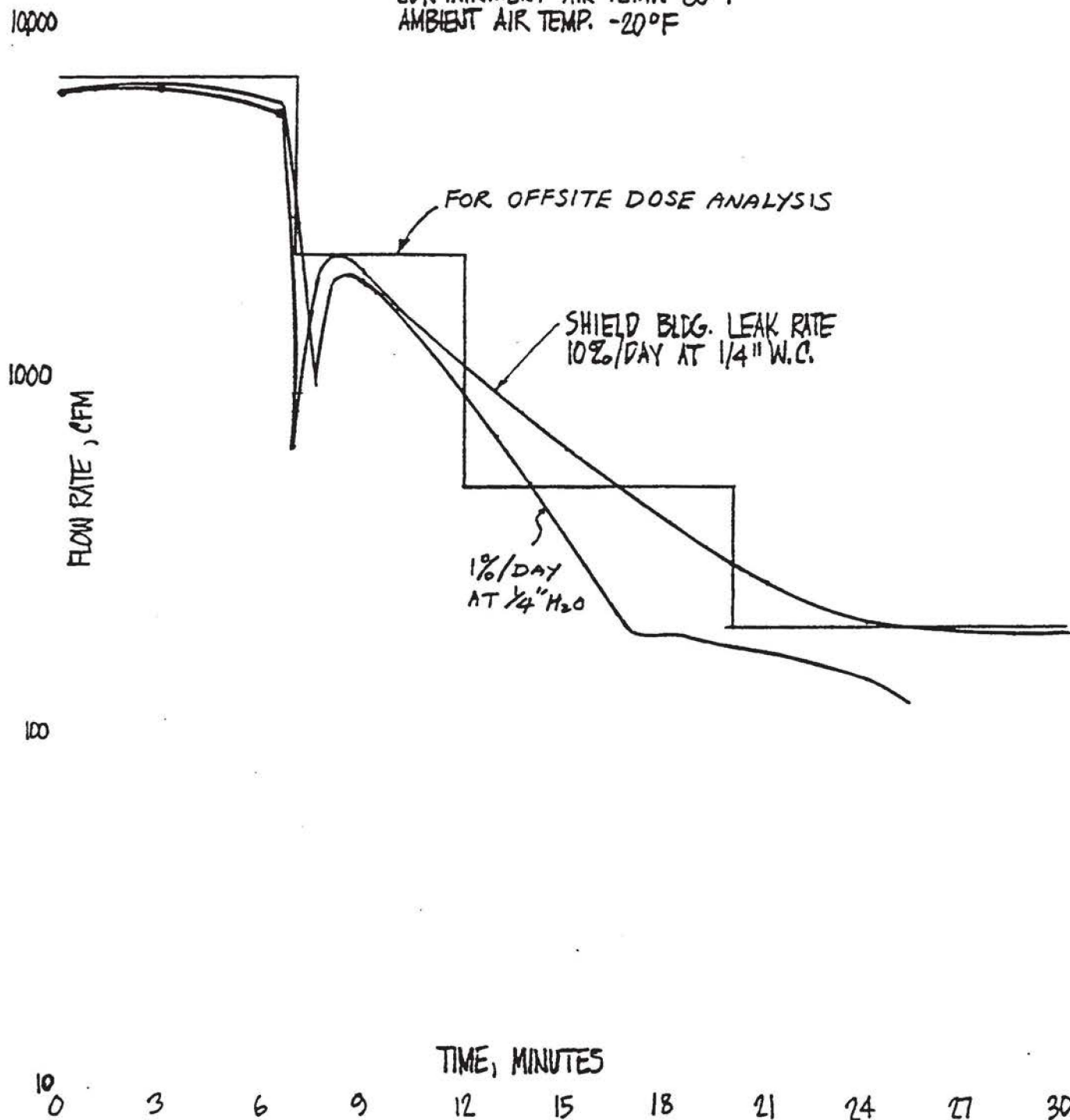


FIGURE G-3-15
PRESSURE TRANSIENT IN THE ANNULUS
I SYSTEM OPERATING

INITIAL AIR TEMP. 60°F
25% HIGHER HEAT TRANSFER TO AIR FROM STEEL SHELL
25% LOWER HEAT TRANSFER TO CONCRETE FROM AIR
WIND EFFECT OF 40 MPH
CONTAINMENT LEAK RATE 1%/DAY
CONTAINMENT AIR TEMP. 80°F
AMBIENT AIR TEMP. -20°F

FIGURE G-3-16
FLOW OUT OF SYSTEM
1 SYSTEMS OPERATING

INITIAL AIR TEMP. 60°F
25% HIGHER HEAT TRANSFER TO AIR FROM STEEL SHELL
25% LOWER HEAT TRANSFER TO CONCRETE FROM AIR
WIND EFFECT 40 MPH
CONTAINMENT LEAK RATE 1%/DAY
CONTAINMENT AIR TEMP. 80°F
AMBIENT AIR TEMP. -20°F



For Wind Pressure

$$q = 0.002558 \times V^2$$

Where q in PSF

V in MPH

For $V = 30$ MPH $q = 2.302$ PSF

$V = 40$ MPH $q = 4.093$ PSF

Max. Pressure = 6.958 PSF = 1.338" W.C.

Aug. Pressure = 3.820 PSF = 0.735" W.C.

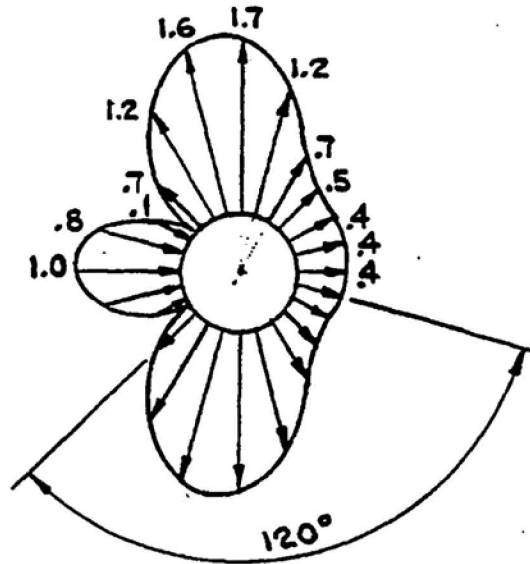


FIGURE G.3-17 - WIND PRESSURE DISTRIBUTION

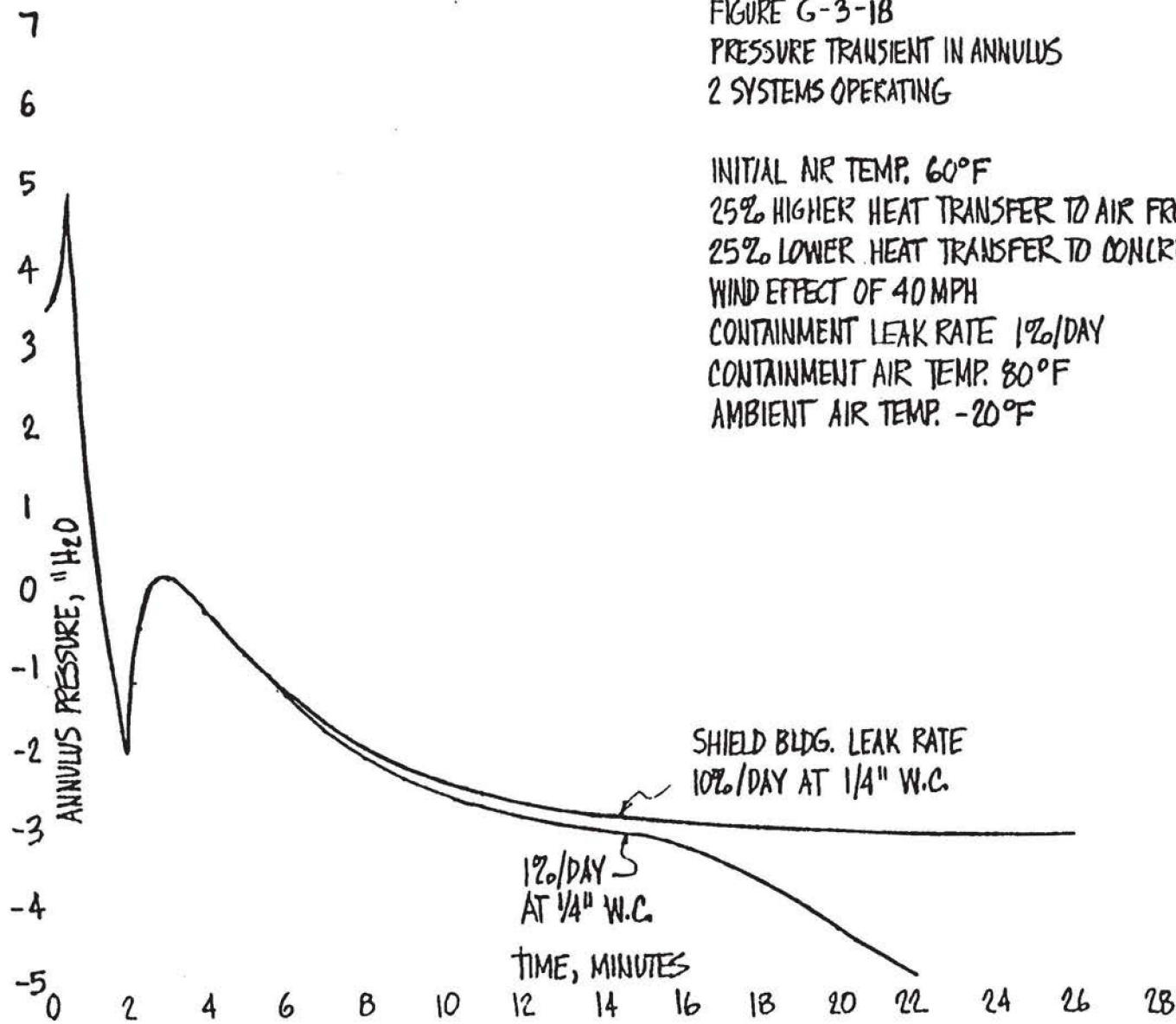
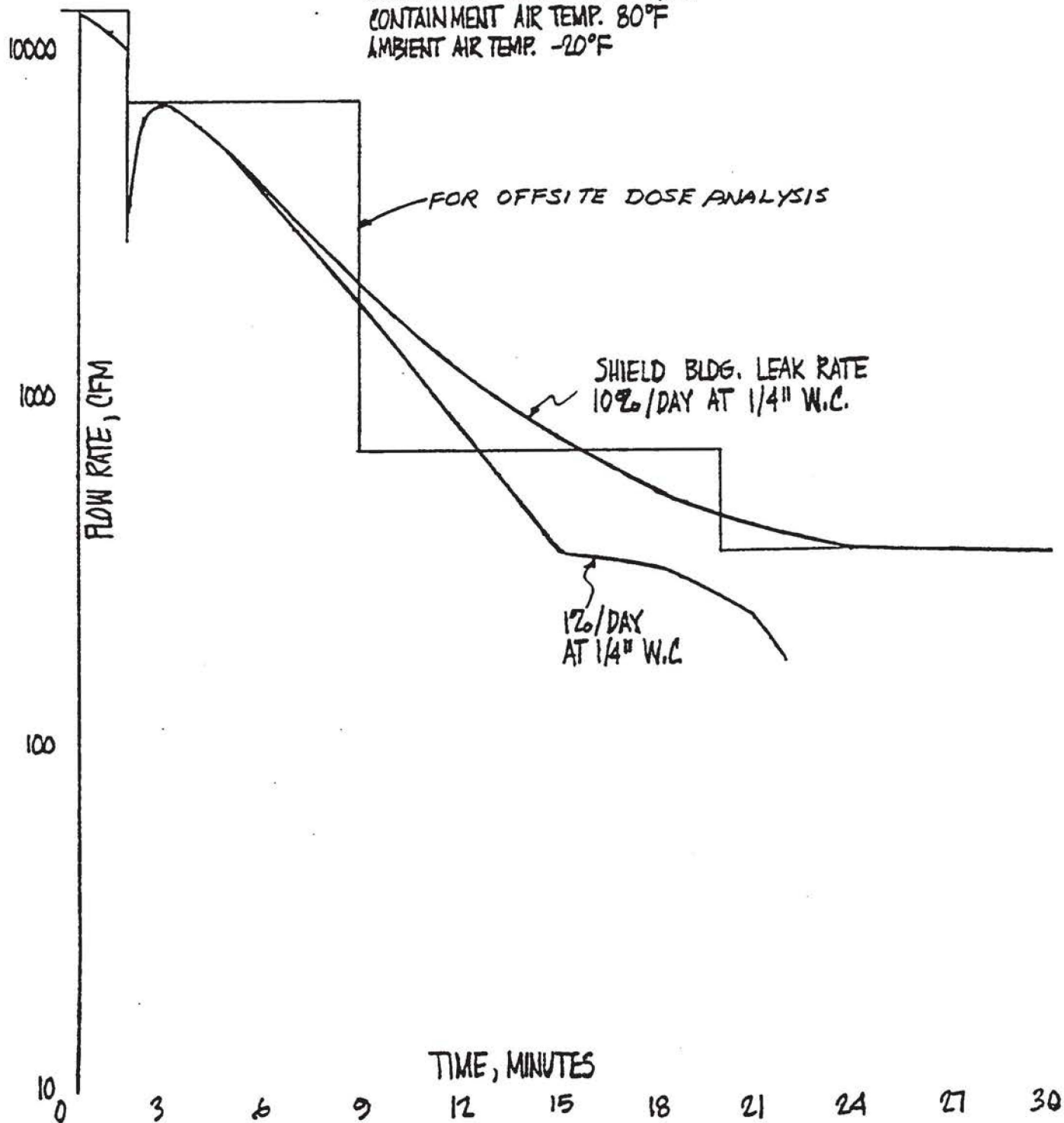


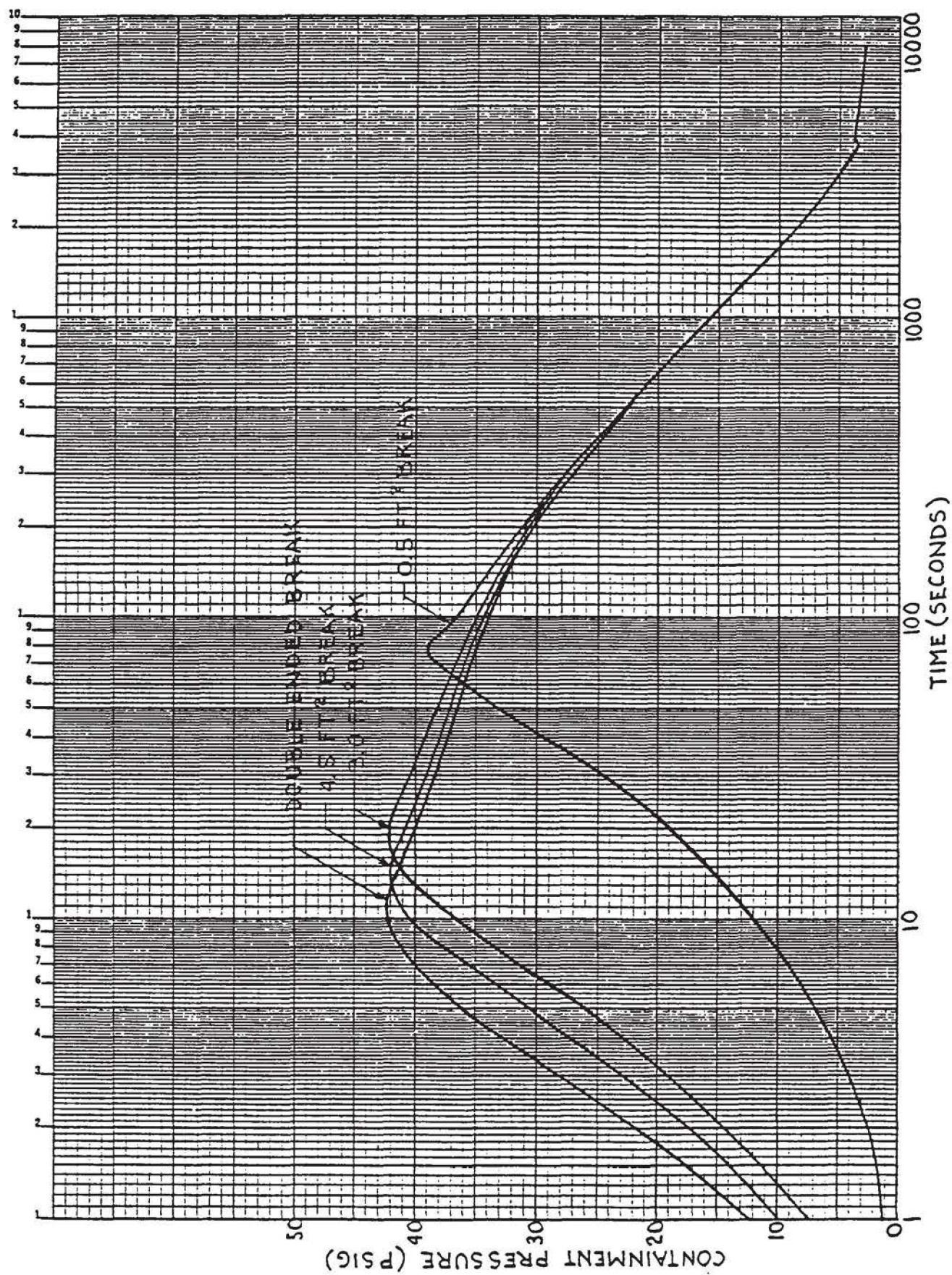
FIGURE G-3-1B
PRESSURE TRANSIENT IN ANNULUS
2 SYSTEMS OPERATING

INITIAL AIR TEMP. 60°F
25% HIGHER HEAT TRANSFER TO AIR FROM STEEL SHELL
25% LOWER HEAT TRANSFER TO CONCRETE FROM AIR
WIND EFFECT OF 40 MPH
CONTAINMENT LEAK RATE 1%/DAY
CONTAINMENT AIR TEMP. 80°F
AMBIENT AIR TEMP. -20°F

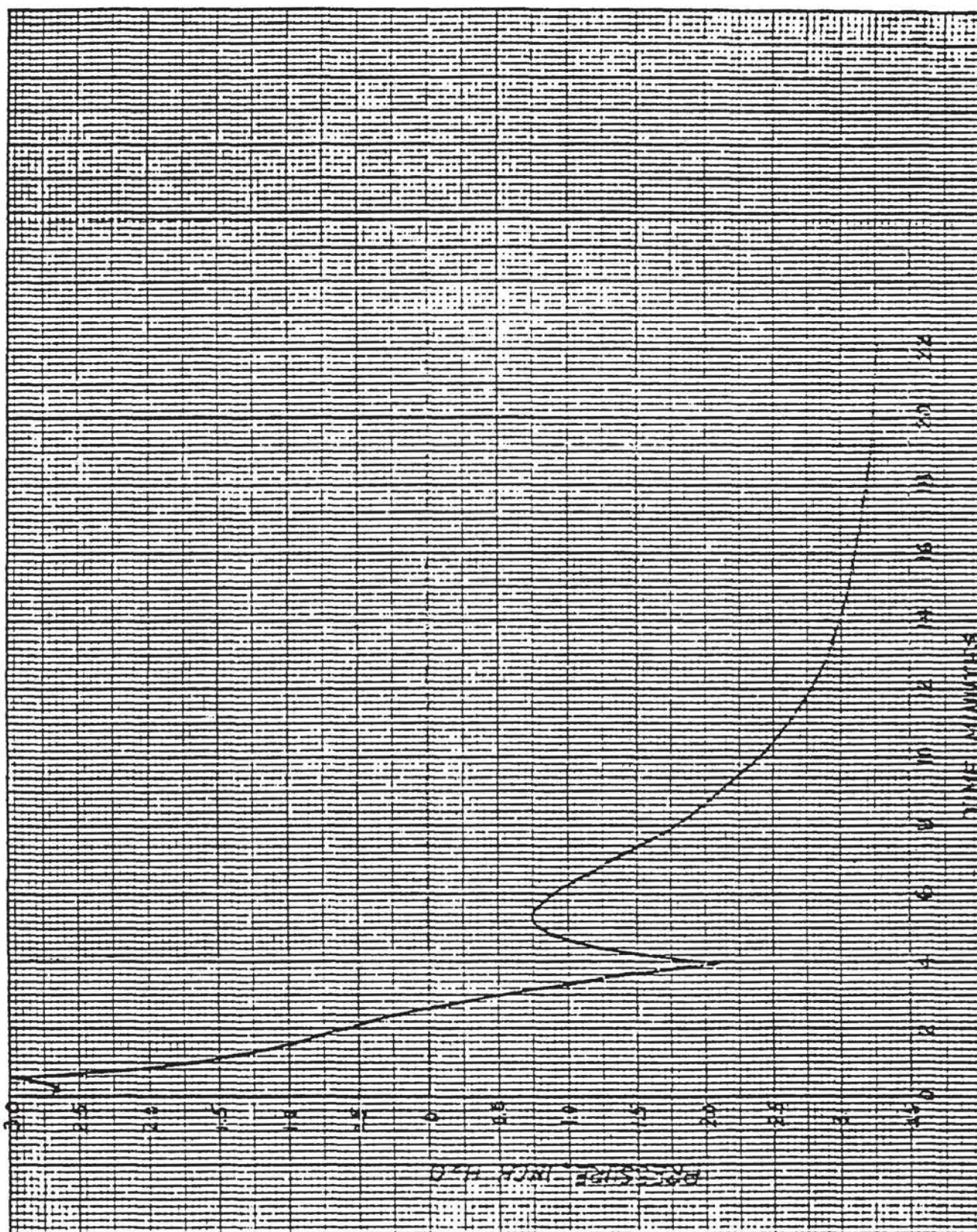
FIGURE G-3-19
FLOW OUT OF SYSTEM
2 SYSTEMS OPERATING

INITIAL AIR TEMP. 60°F
25% HIGHER HEAT TRANSFER TO AIR FROM STEEL SHELL
25% LOWER HEAT TRANSFER TO CONCRETE FROM AIR
WIND EFFECT 40 MPH
CONTAINMENT LEAK RATE 1%/DAY
CONTAINMENT AIR TEMP. 80°F
AMBIENT AIR TEMP. -20°F

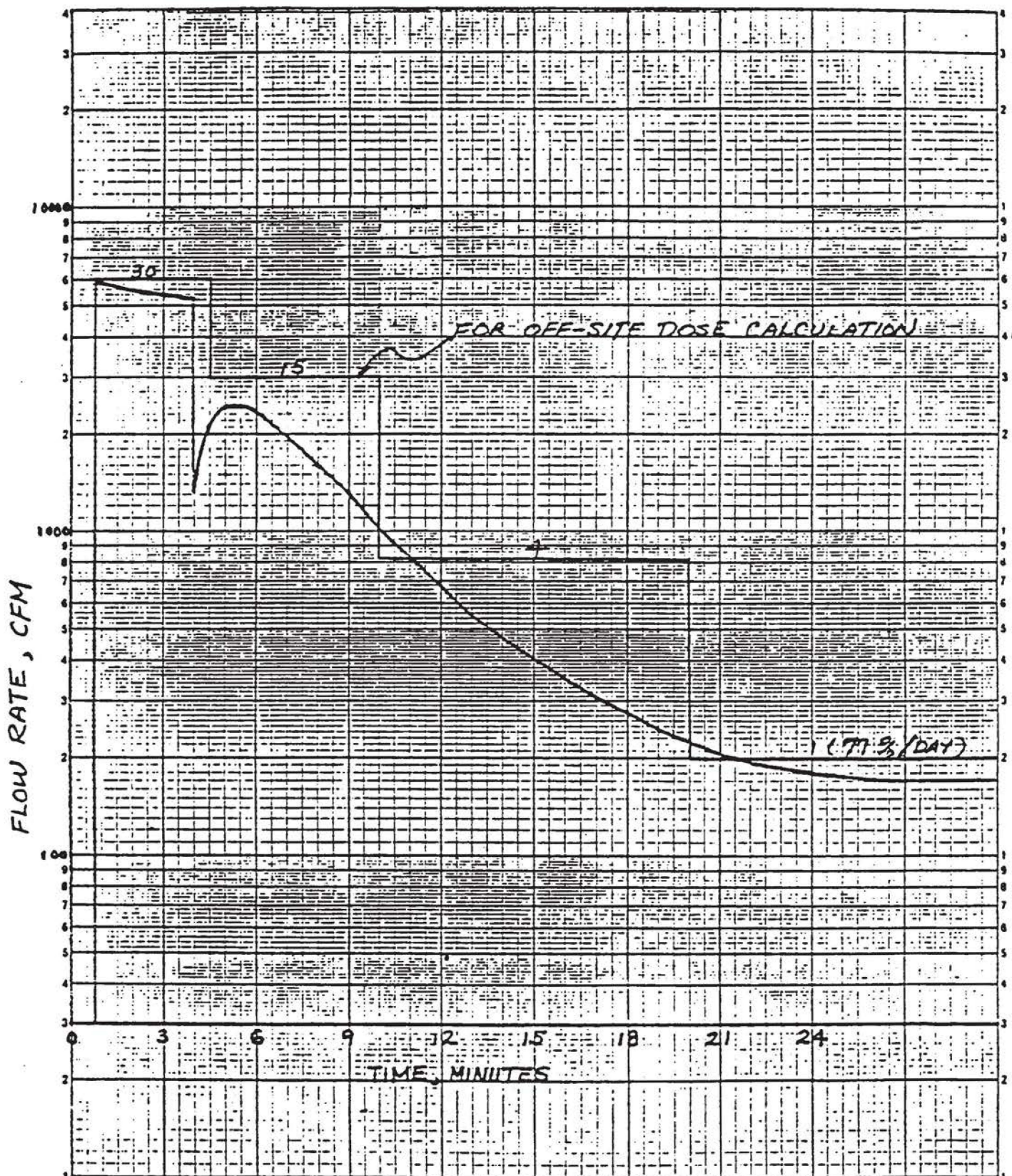




CONTAINMENT PRESSURE TRANSIENT
FIGURE G.3-20 REV 4 12/85

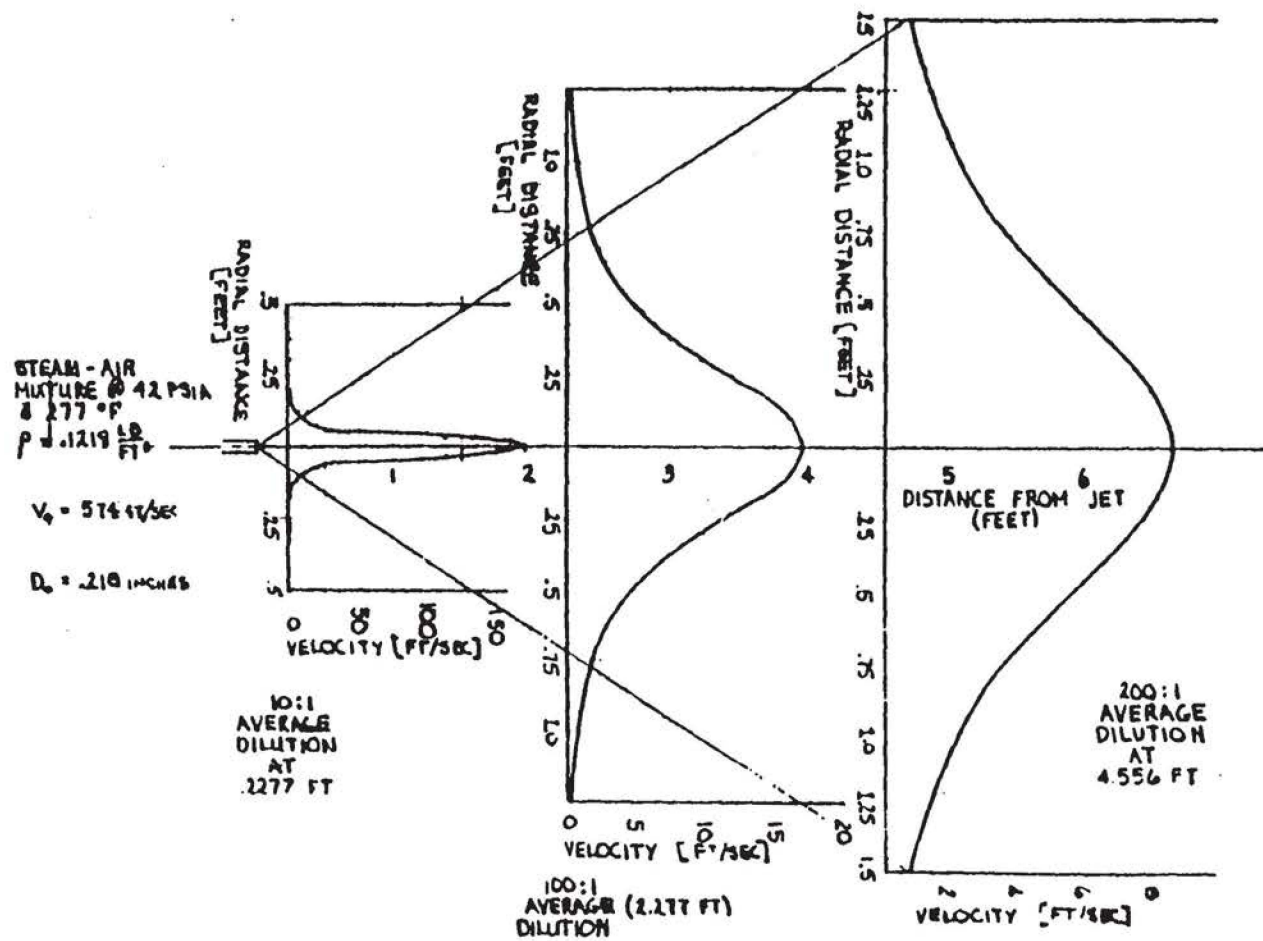


ANNULUS PRESSURE
 DESIGN BASIS TRANSIENT
 FIGURE G.3-21 REV 4 12/85



FLOW OUT OF SBVS
DESIGN BASIS TRANSIENT
FIGURE G.3-22

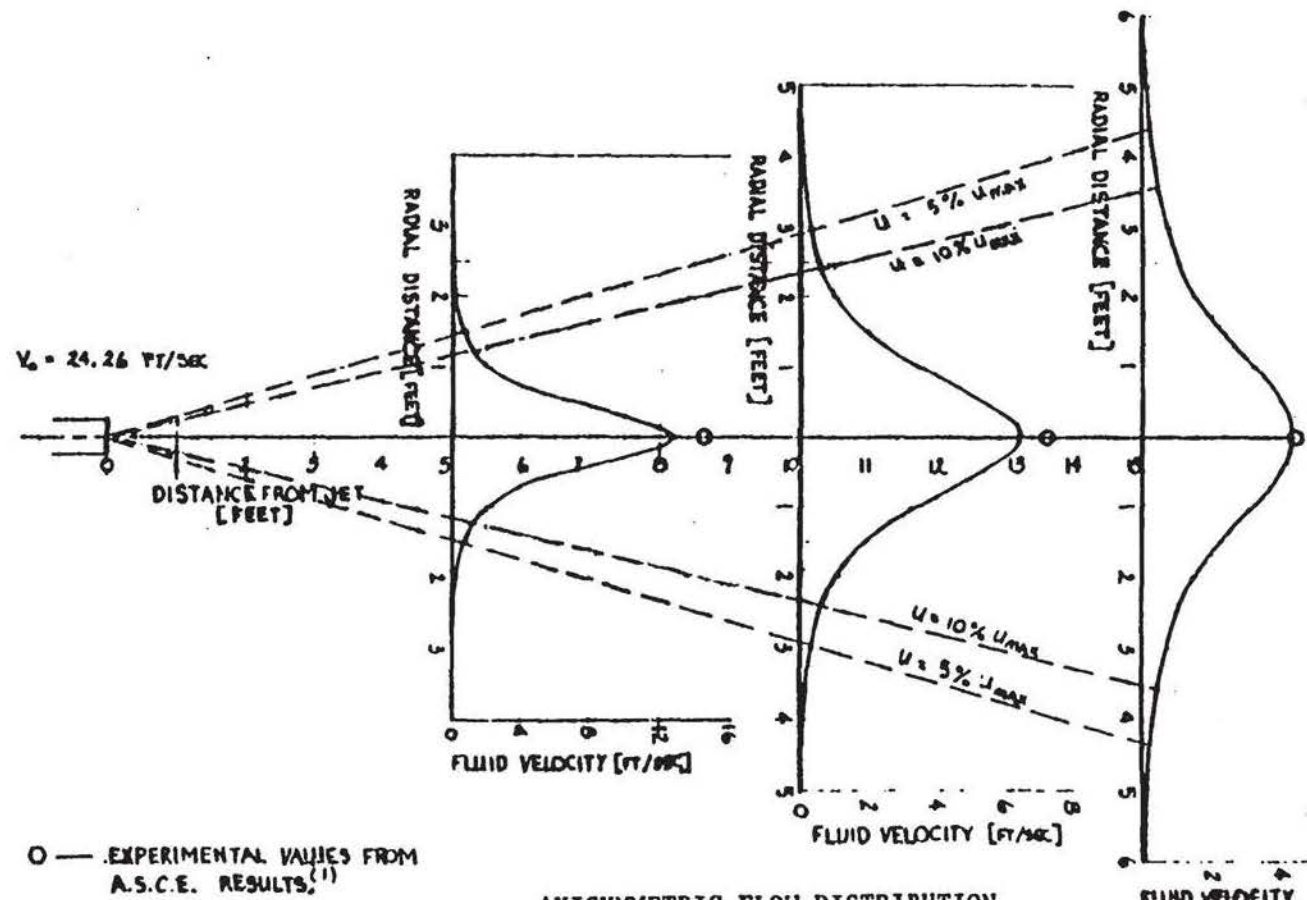
REV 4 12/85



AXISYMMETRIC FLOW DISTRIBUTION
FROM A CIRCULAR JET

FIGURE G.5-1

REV 4 12/85



AXISYMMETRIC FLOW DISTRIBUTION
FROM A CIRCULAR JET

FIGURE G.5-2